A

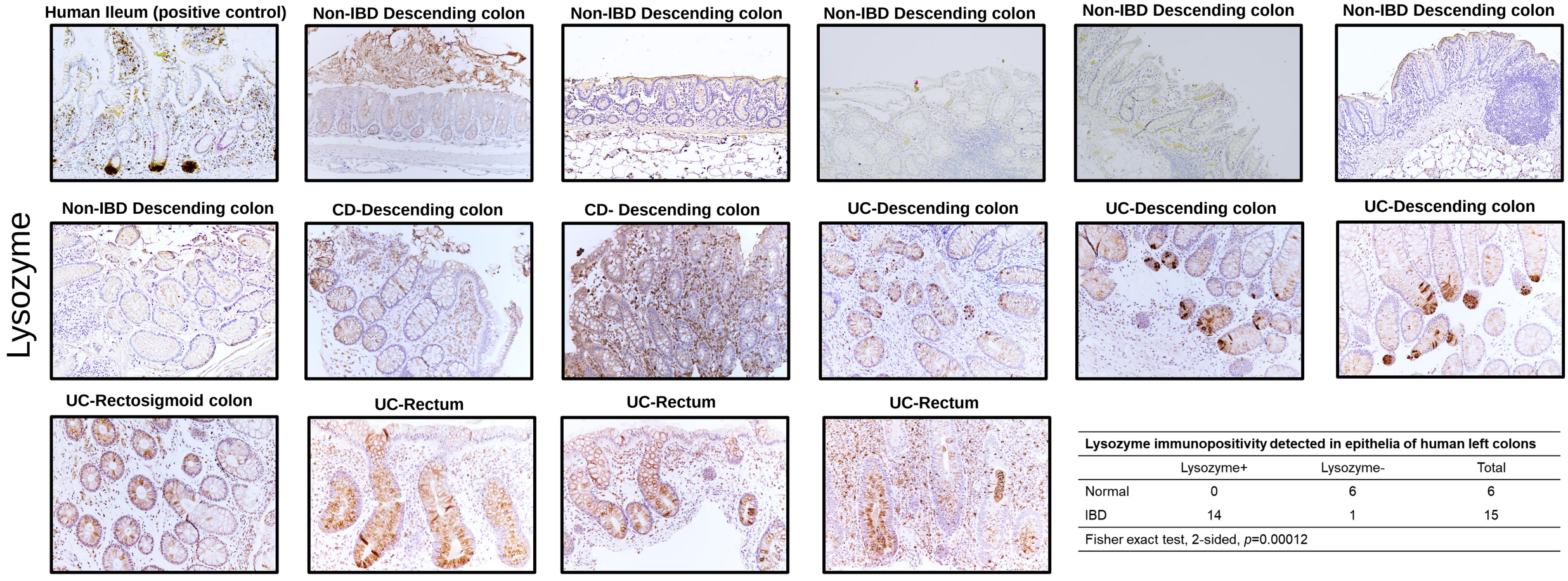

Lysozyme immunopositivity detected in epithelia of human left colons			
	Lysozyme+	Lysozyme-	Total
Normal	0	6	6
IBD	14	1	15
Fisher exact test, 2-sided, p=0.00012			

B

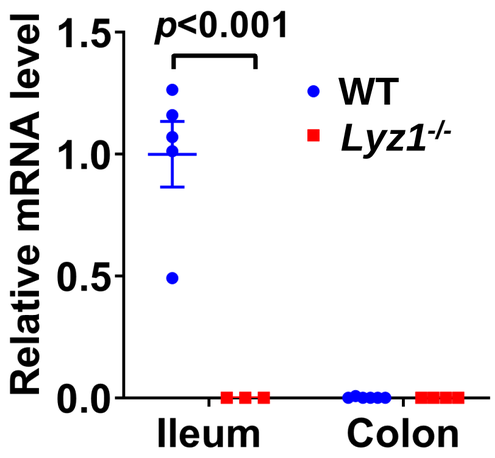

C

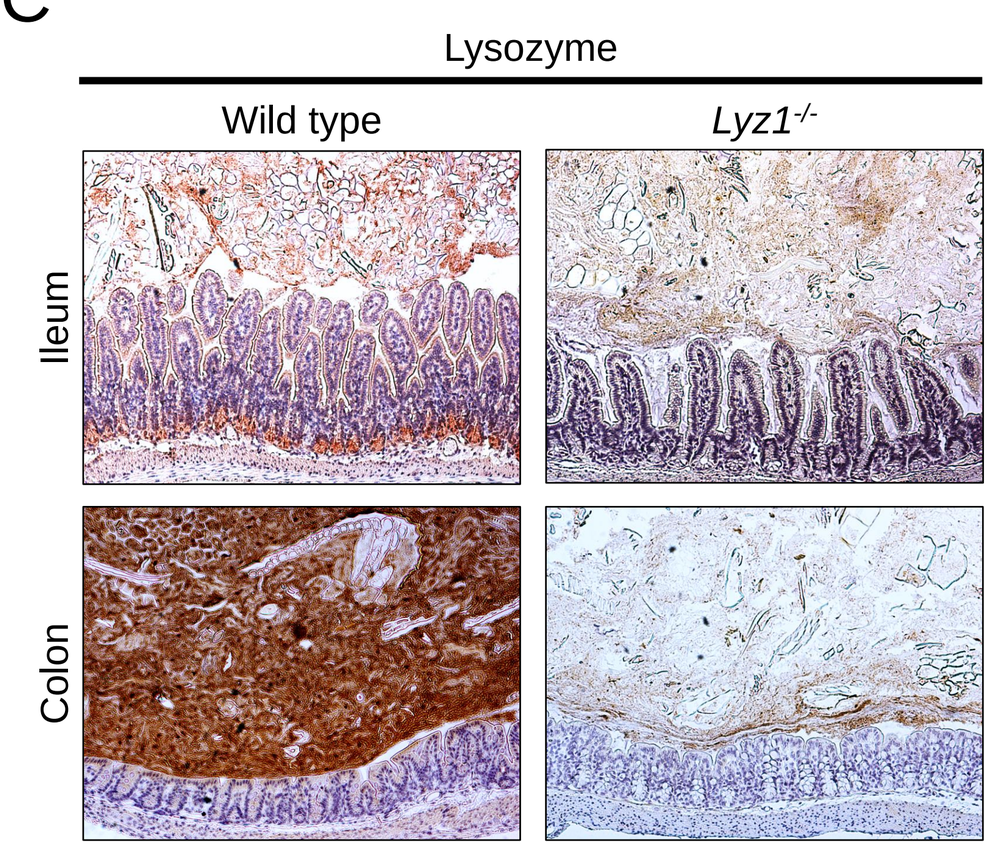

D

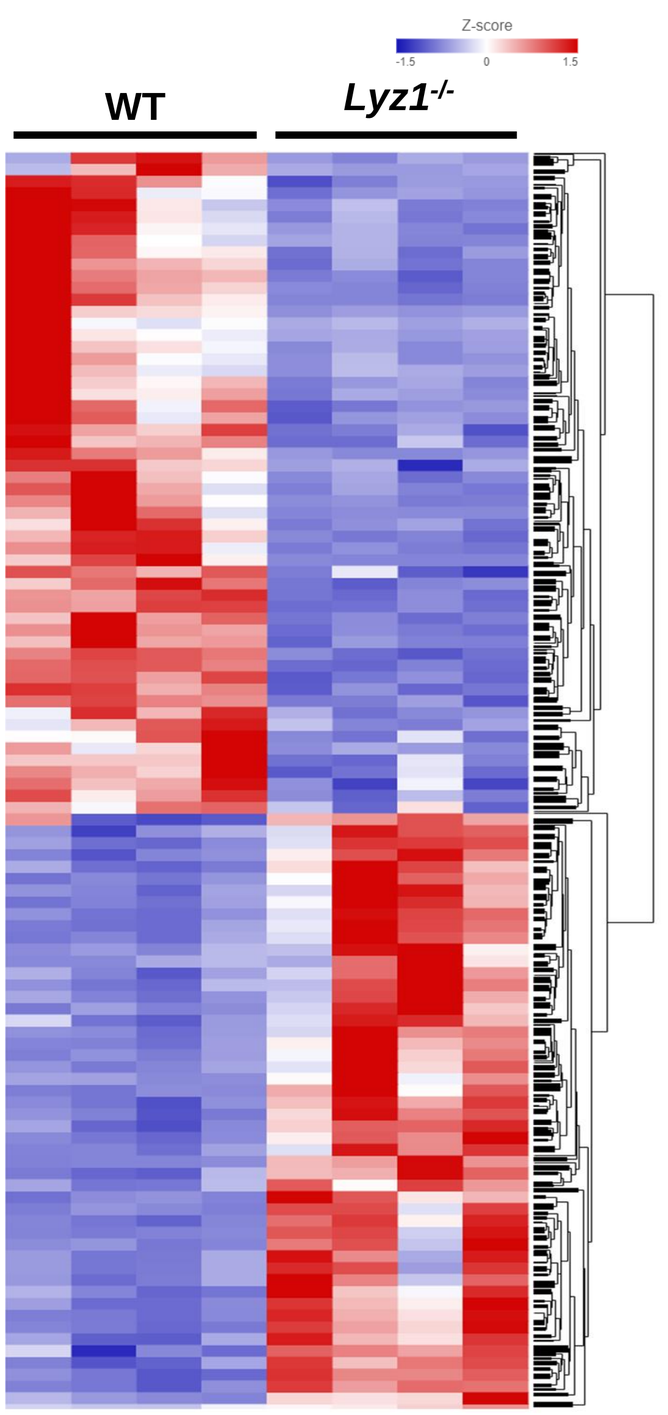

E

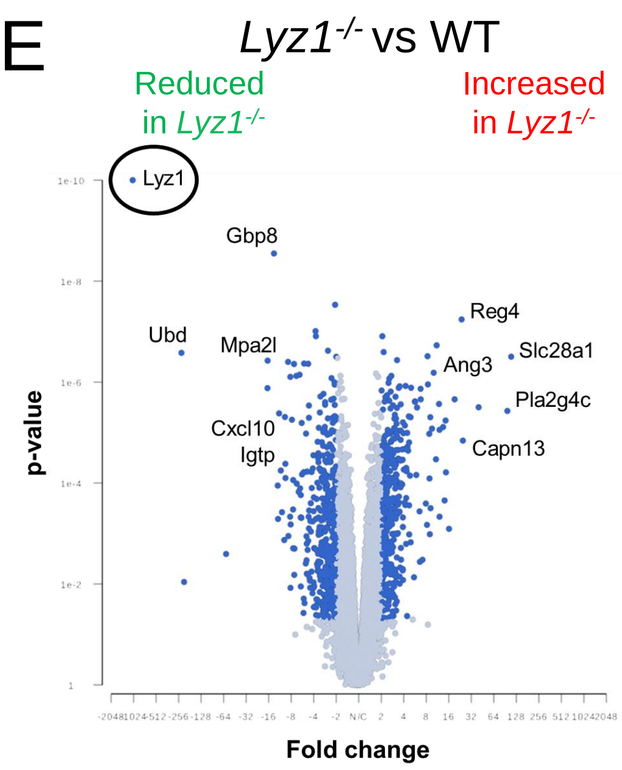

F

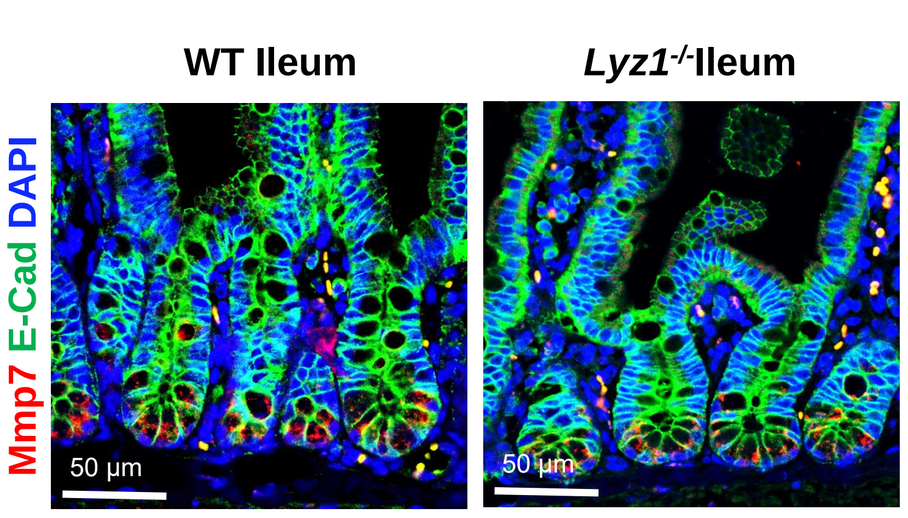

G

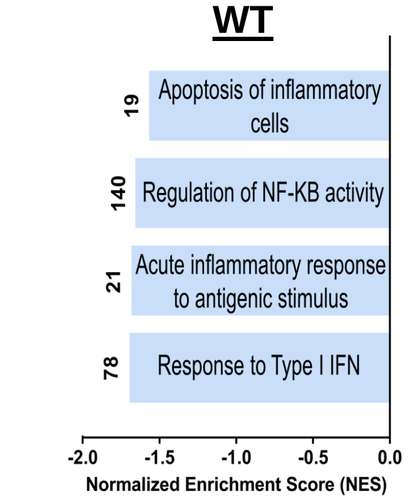

H

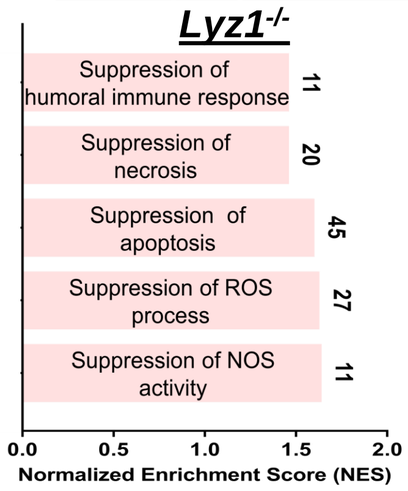

I

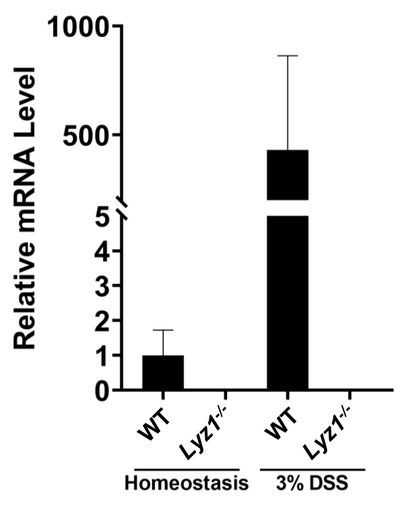

J

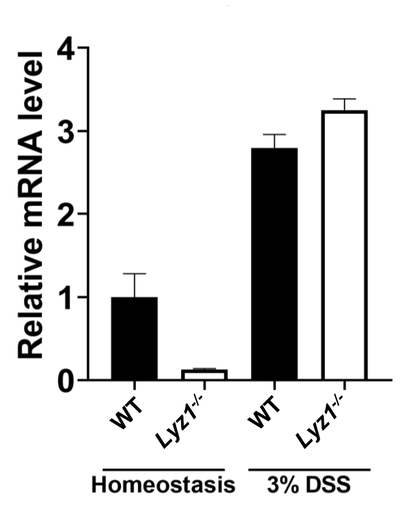

K

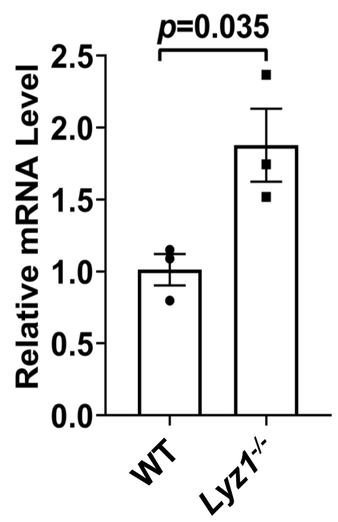

Fig. S1. *Lyz1* deficiency reduces inflammation during experimental colitis, Related to Figure 1.
(A) 15 IBD pathology cases of indicated anatomic region and 6 non-IBD colon tissues were stained for lysozyme to identify lysozyme-positive metaplastic Paneth cells. **(B)** qPCR analysis of Lyz1 mRNA in WT and *Lyz1*$^{-/-}$ ileum and colon (N=3-5 mice for each genotype). **(C)** Representative immunostaining of lysozyme in the ileum and colon of WT and *Lyz1*$^{-/-}$ mice (N=3 mice per genotype). **(D)** Differential expression of genes in WT and *Lyz1*$^{-/-}$ ileum (N=4 mice per genotype). **(E)** Volcano plot of differentially expressed genes in WT and *Lyz1*$^{-/-}$ ileum. Blue color: genes with fold change < -2 or > 2; p-value < 0.05 (N= 4 mice per genotype). **(F)** Immunostaining of Mmp7 in WT and *Lyz1*$^{-/-}$ ileum (N=3 mice per genotype). **(G)** GSEA of RNA-seq data revealed an increase in the pathways mentioned in WT ileum. Numbers above the bar graphs represent the number of genes from the WT dataset included within the GSEA gene set (N=4 mice). **(H)** Gene ontology analysis of RNA-seq data revealed gene sets upregulated in *Lyz1*$^{-/-}$ ileum. Numbers above the bar graphs represent the number of genes from the *Lyz1*$^{-/-}$ dataset included within the GSEA gene set (N=4 mice). **(I, J)** Real-time PCR analysis of Lyz1 **(I)** and Lyz2 **(J)** displayed induction of these genes in inflamed colon tissues of WT mice. In KO mice, only Lyz2 was induced in DSS-treated WT and *Lyz1*$^{-/-}$ mouse colons (N=3-6 mice per genotype per condition). **(K)** Real-time PCR analysis of Areg in DSS-treated *Lyz1*$^{-/-}$ colons (N=3 mice per genotype). All bar graphs display mean ± SEM.

A

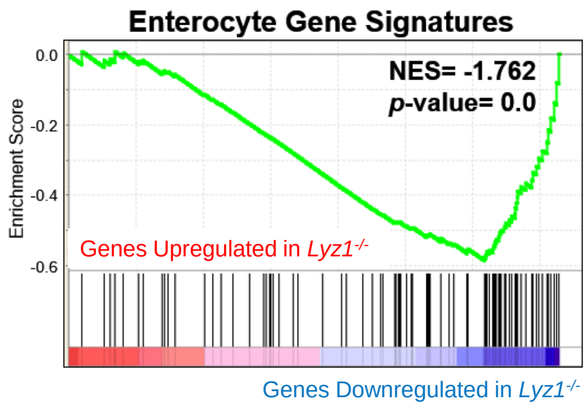

B

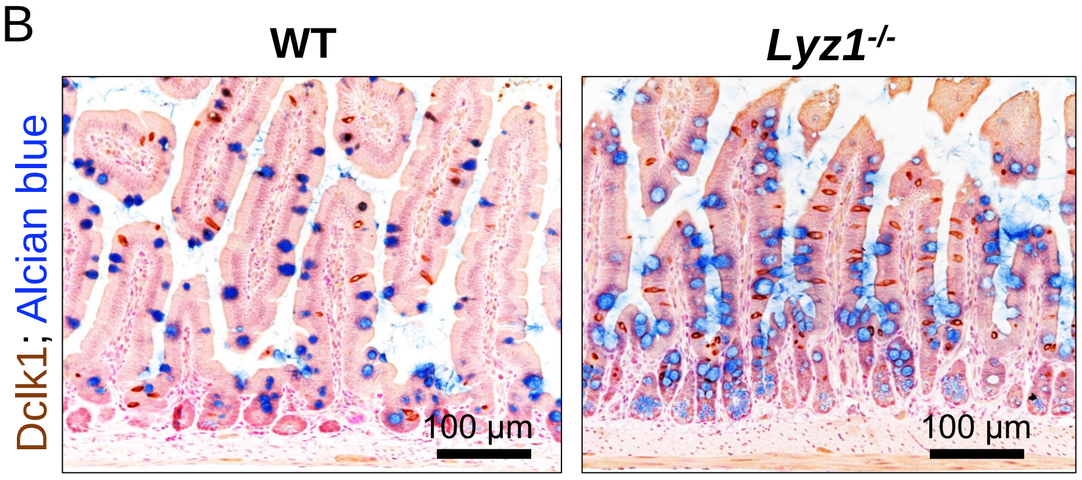

C

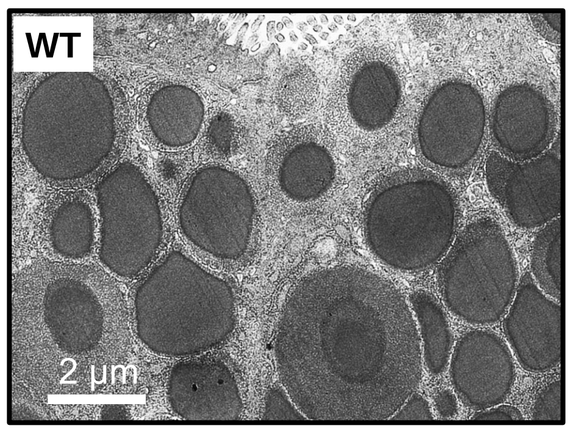

D

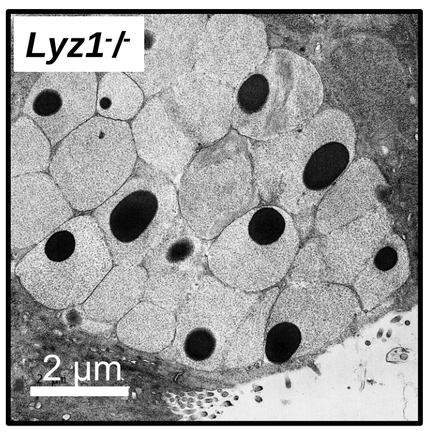

E

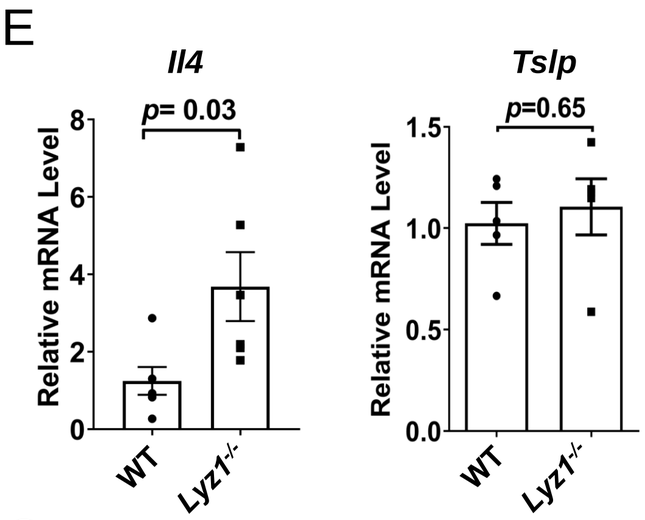

F

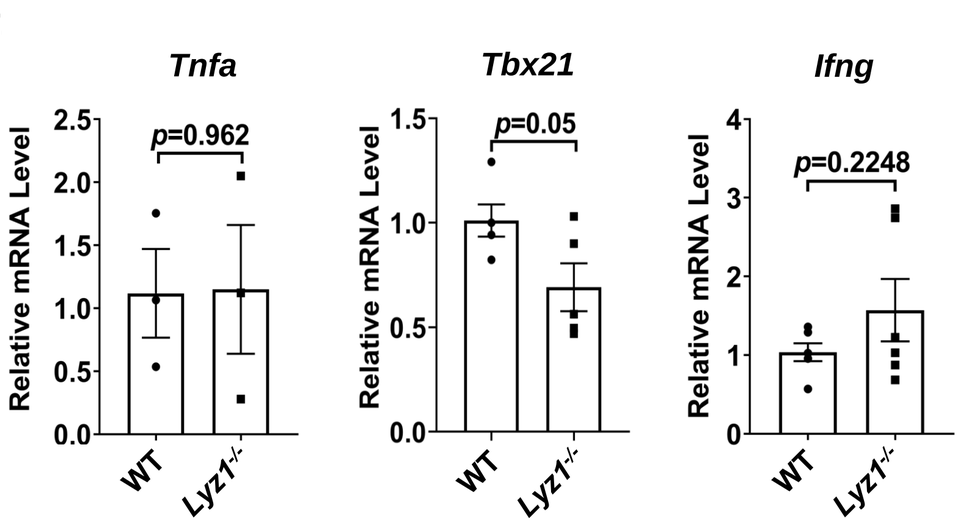

G

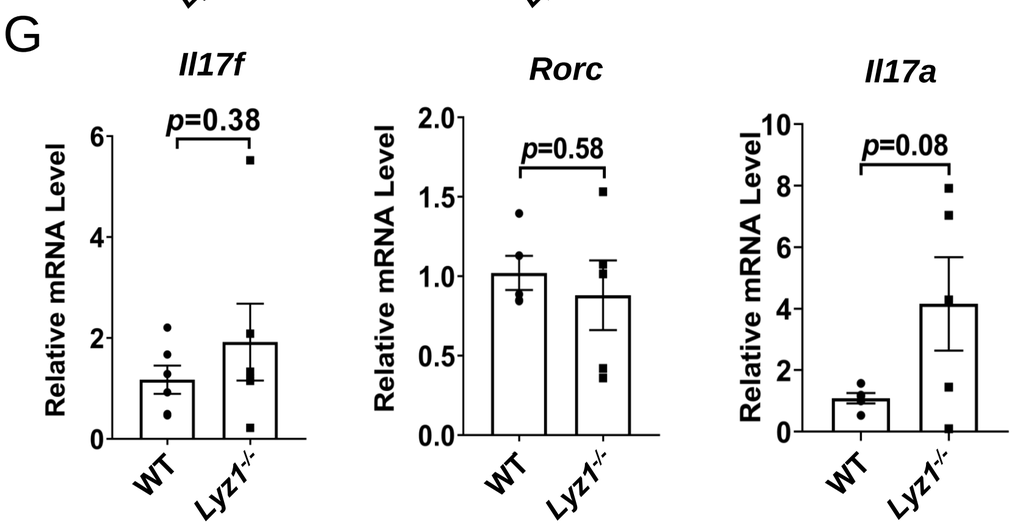

H

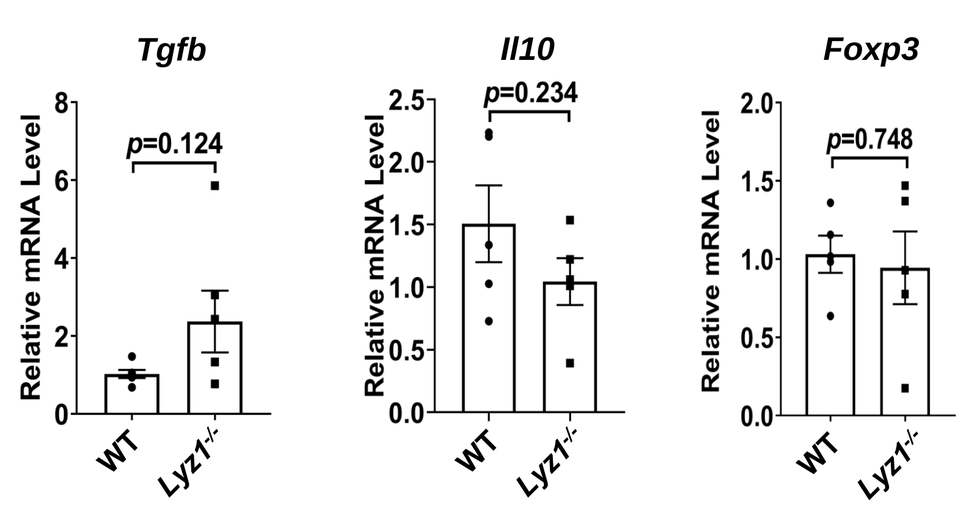

I

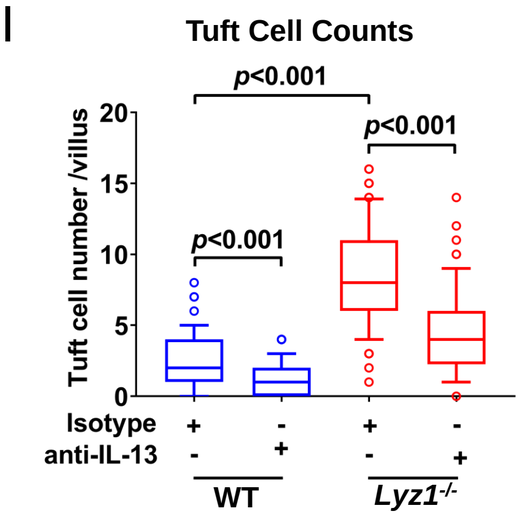

J

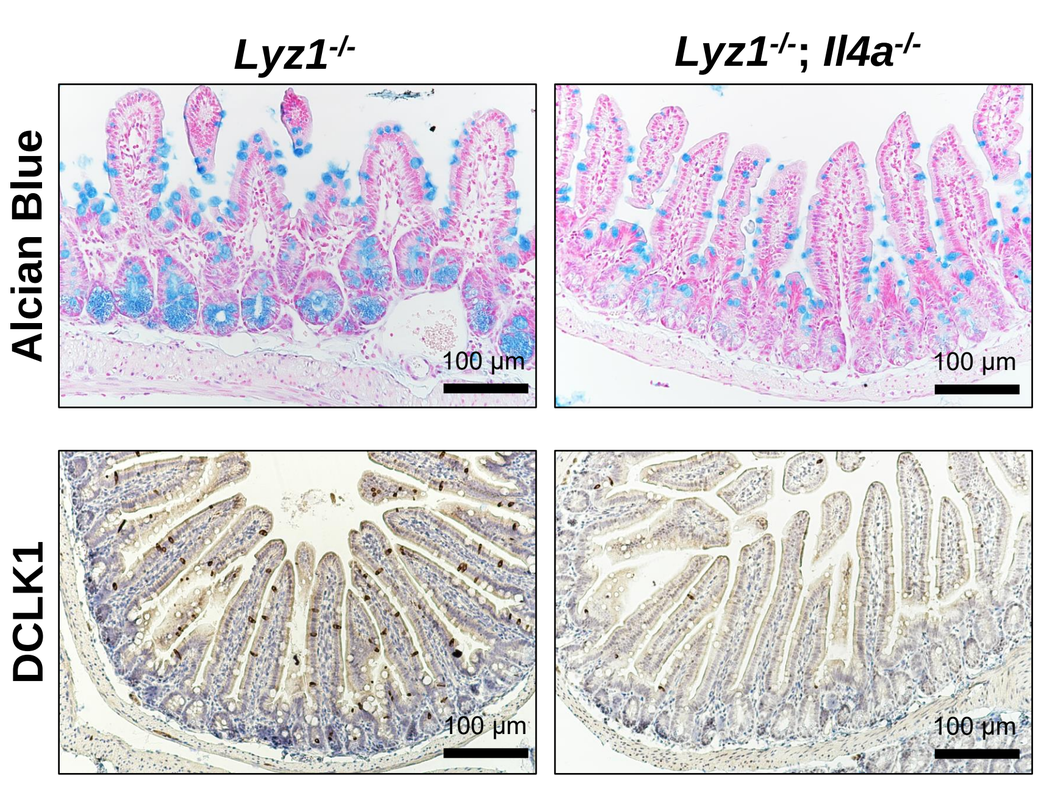

K

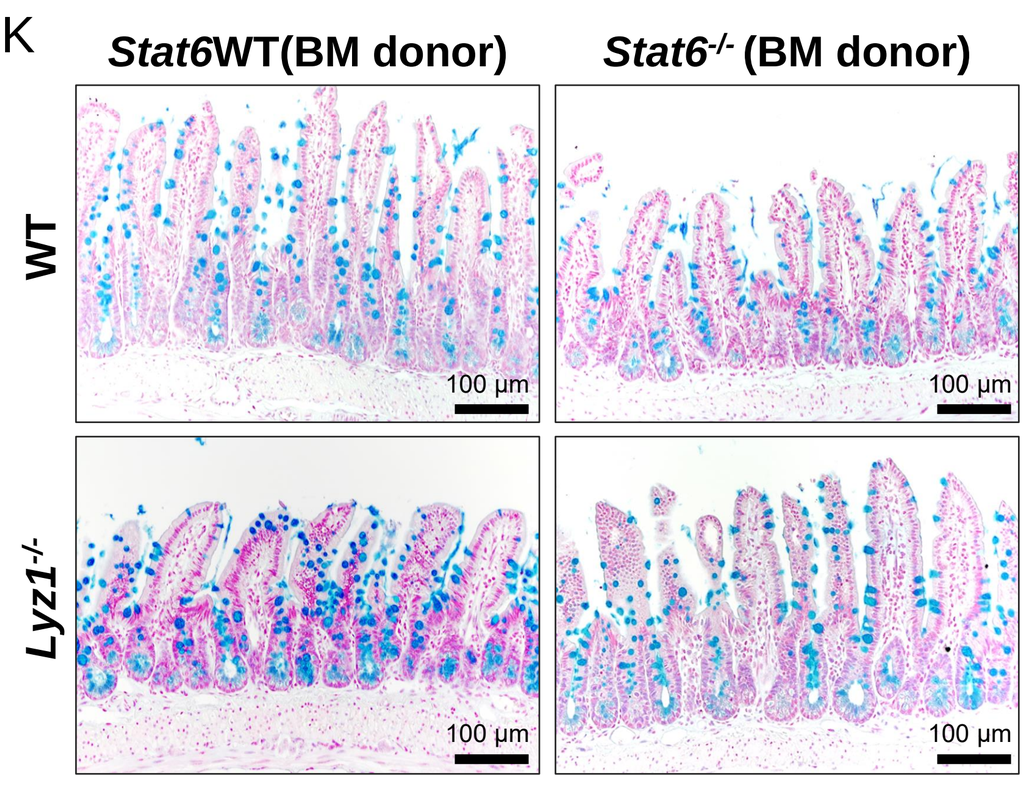

Fig. S2. *Lyz1*$^{-/-}$ intestines have increased goblet and tuft cells, Related to Figure 2.
(A) GSEA analysis of RNA-seq data (N=4 mice per genotype) comparing enterocyte gene signature in WT and *Lyz1*$^{-/-}$ ileum. **(B)** Immunostaining of Alcian blue and Dclk1 in WT and *Lyz1*$^{-/-}$ intestines (N=5 mice per genotype; 3 independent experiments). **(C, D)** Transmission electron microscopy of a cell with granules characteristic of mixed Paneth and goblet cell morphologies at the crypt base in the *Lyz1*$^{-/-}$ ileum **(C)** when compared to the Paneth cell observed at the crypt base of WT ileum**(D)** (N=3 mice per genotype). **(E-H)** Real-time PCR analysis of genes associated with type 2 **(E),** type 1 **(F)**, type 3 **(G)**, or regulatory **(H)** immune response in WT and *Lyz1*$^{-/-}$ mice (N=3-6 mice per genotype). **(I)** Tuft cell numbers (counted from 50 villi per field of vision per mouse) in WT or *Lyz1*$^{-/-}$ mice treated with neutralizing anti-IL-13 antibody, anti-CD90.2, or isotype control (N=2 for each condition per genotype). **(J)** Representative Alcian blue (goblet) and DCLK1 (tuft) staining in *Lyz1*$^{-/-}$ and *Lyz1*$^{-/-}$;*Il4ra*$^{-/-}$ mice (N=3 mice per genotype). Data is representative of 50-80 villi per section per mouse per genotype. **(K)** Alcian blue staining of WT or *Lyz1*$^{-/-}$ bone marrow chimeras with hematopoietic cells from Stat6$^{+/+}$ or Stat6$^{-/-}$ donors (N=4 mice per genotype per treatment; 2 independent experiments). All bar graphs display mean ± SEM.

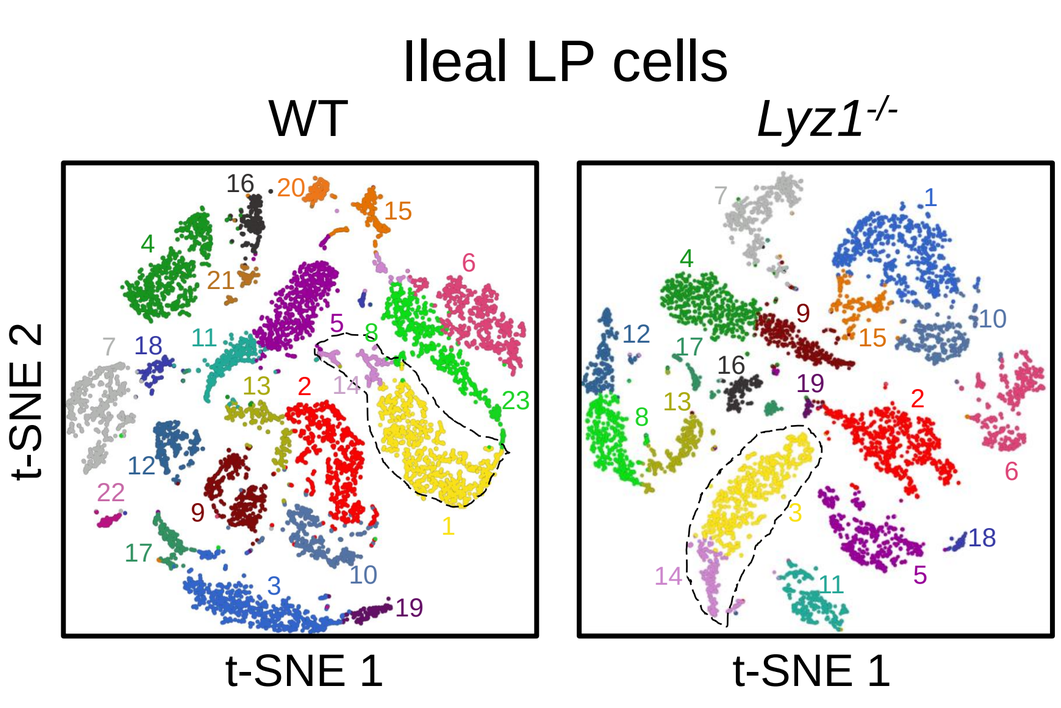
A
Ileal LP cells
WT
Lyz1-/-
t-SNE 2
t-SNE 1
t-SNE 1

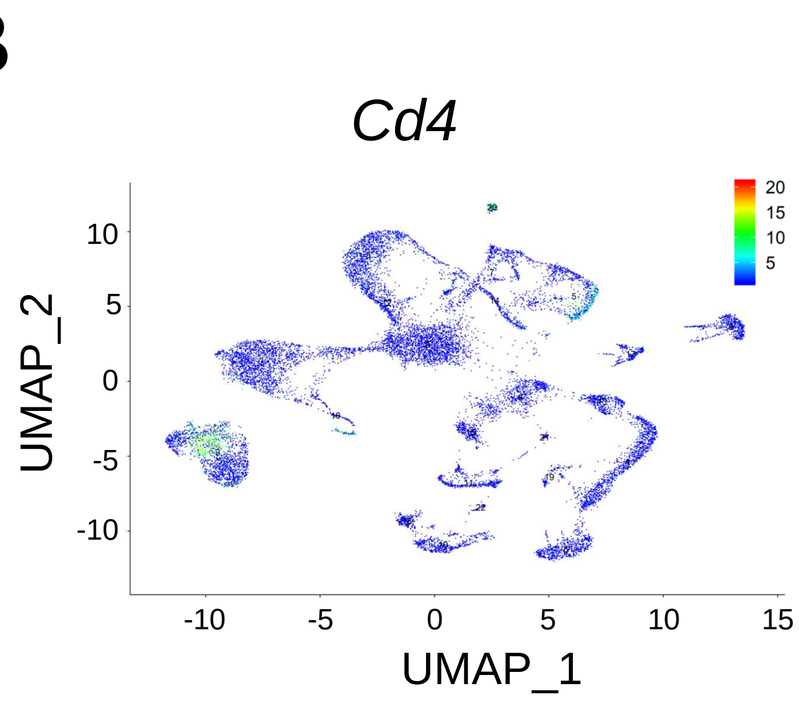
B
Cd4
UMAP_2
UMAP_1
20
15
10
5

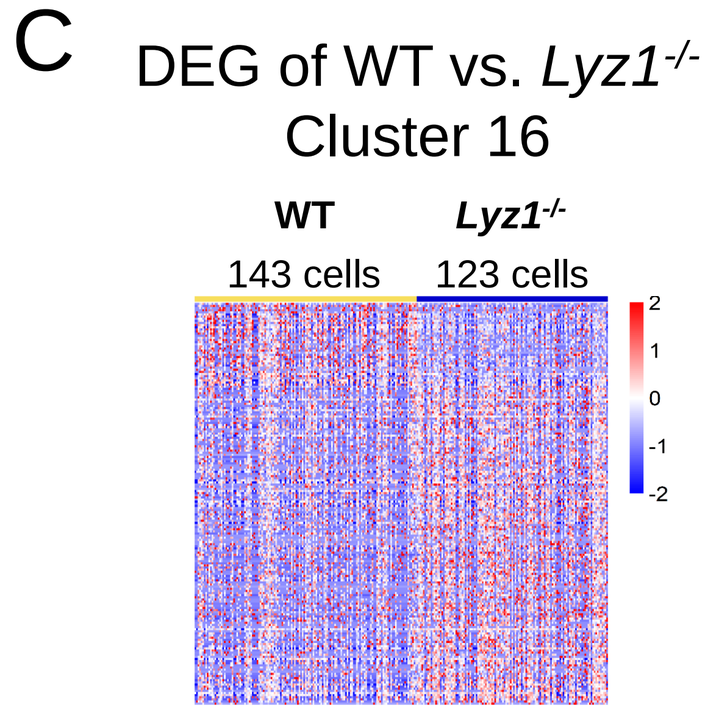
C
DEG of WT vs. Lyz1-/-
Cluster 16
WT
Lyz1-/-
143 cells
123 cells
2
1
0
-1
-2

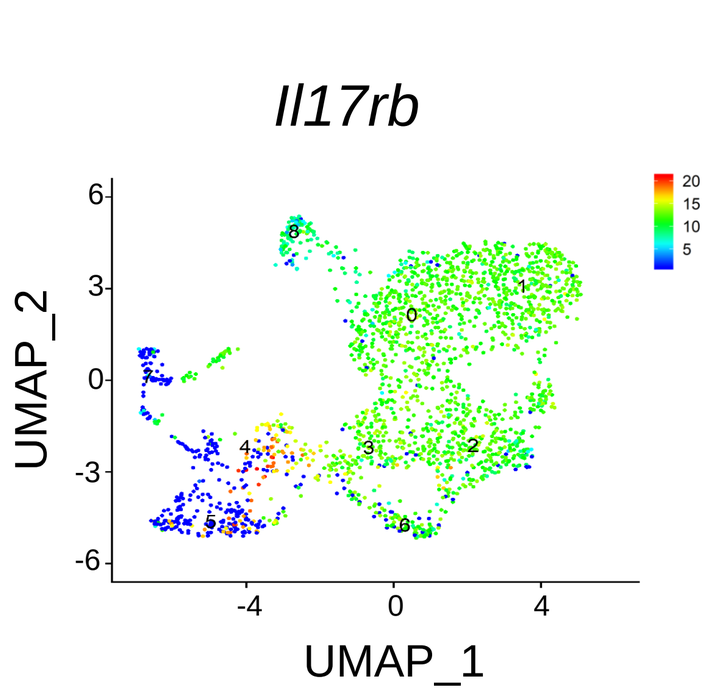
D
Il17rb
UMAP_2
UMAP_1
20
15
10
5

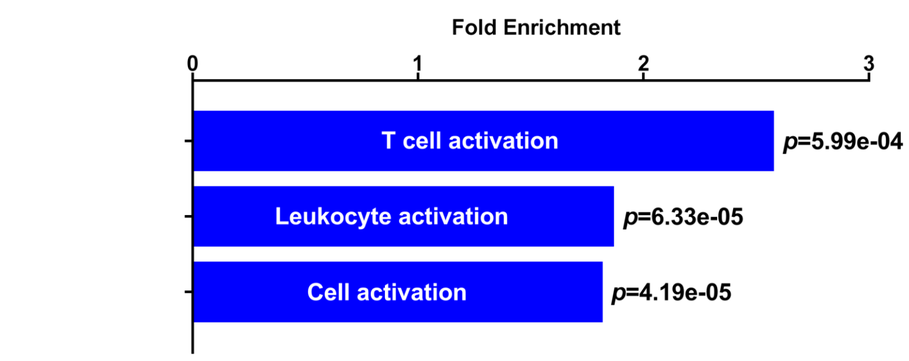
E
Gene Ontology
(Upregulated in Lyz1-/- Cluster 16)
Fold Enrichment
T cell activation
p=5.99e-04
Leukocyte activation
p=6.33e-05
Cell activation
p=4.19e-05

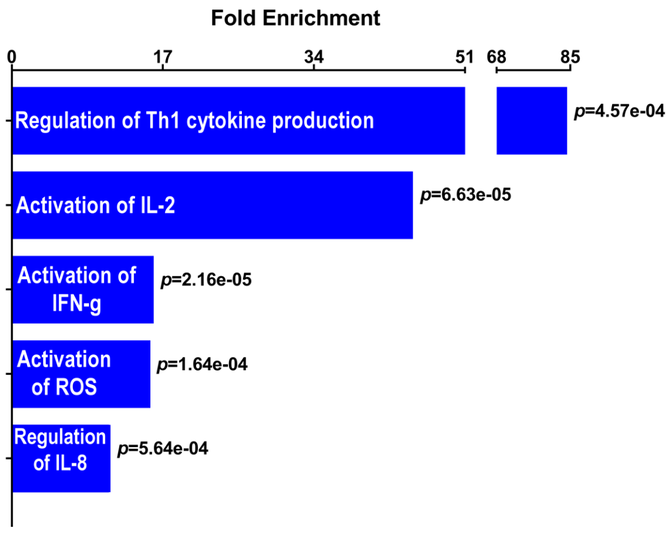
F
Gene Ontology
(Upregulated in WT Cluster 16)
Fold Enrichment
Regulation of Th1 cytokine production
p=4.57e-04
Activation of IL-2
p=6.63e-05
Activation of IFN-g
p=2.16e-05
Activation of ROS
p=1.64e-04
Regulation of IL-8
p=5.64e-04

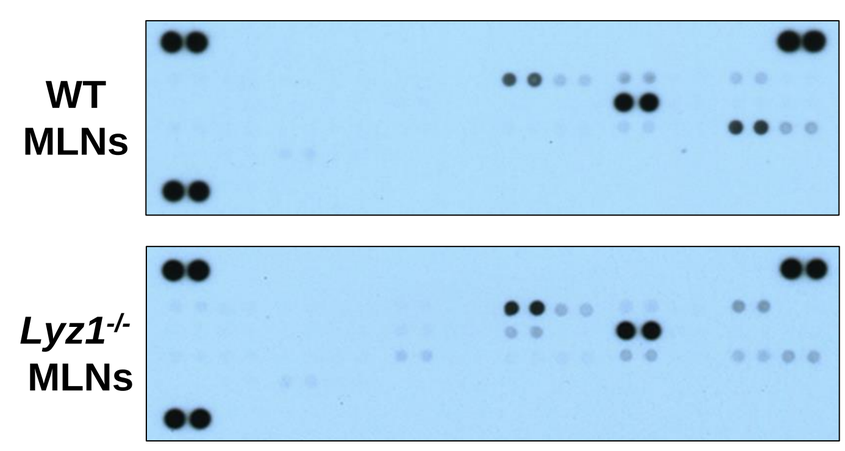
G
WT MLNs
Lyz1-/- MLNs

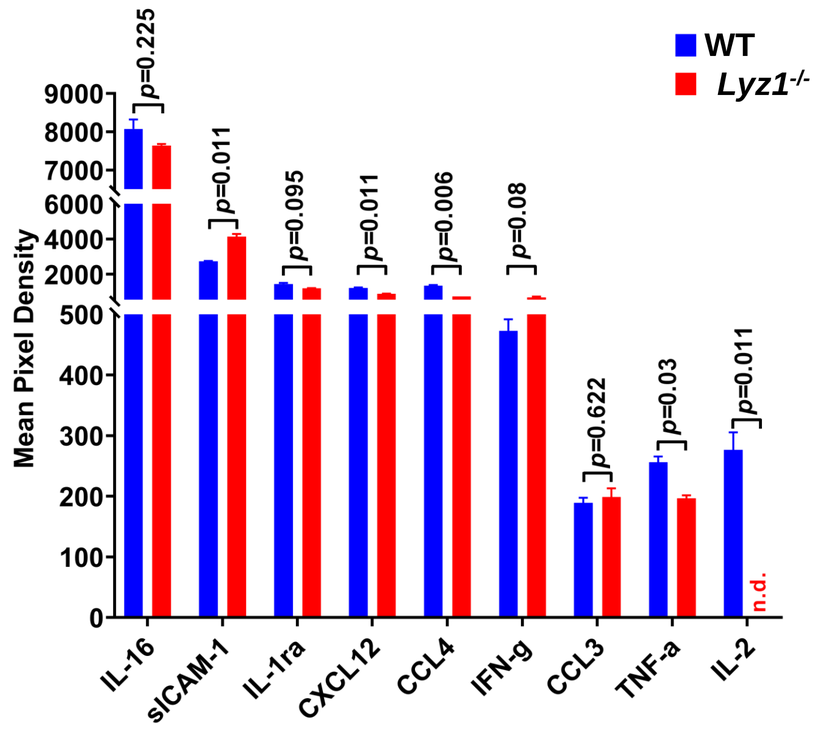
H
WT
Lyz1-/-
Mean Pixel Density
p=0.225
p=0.011
p=0.095
p=0.011
p=0.006
p=0.08
p=0.622
p=0.03
p=0.011
n.d.
IL-16
sICAM-1
IL-1ra
CXCL12
CCL4
IFN-g
CCL3
TNF-a
IL-2

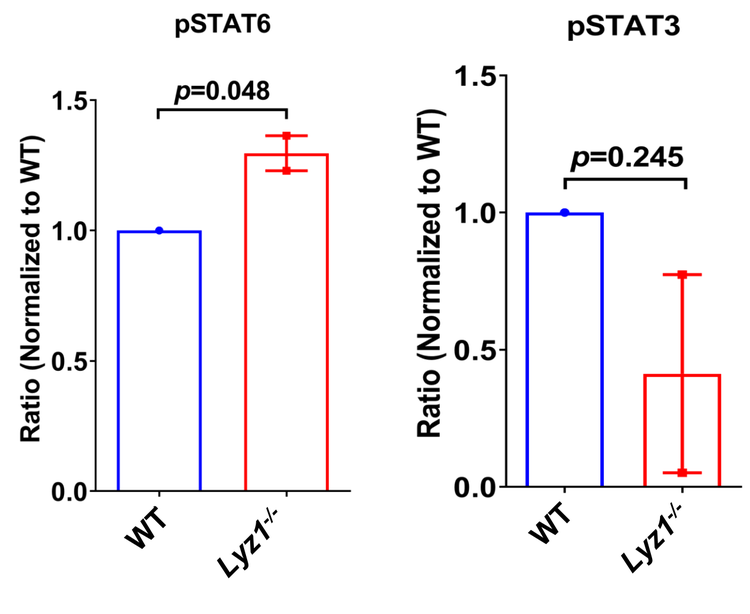
I
pSTAT6
p=0.048
Ratio (Normalized to WT)
WT
Lyz1-/-
pSTAT3
p=0.245
Ratio (Normalized to WT)
WT
Lyz1-/-

Fig. S3. scRNAseq reveals immune-activated ILC2 in *Lyz1*$^{-/-}$ ileal lamina propria, Related to Figure 3

(A)) Unsupervised separate clustering (t-SNE plot) of 8,011 WT LP and 6,733 *Lyz1*$^{-/-}$ LP cells identified 23 and 19 distinct clusters, respectively. **(B-D)** Combined clustering of WT and *Lyz1*$^{-/-}$ ileal LP cells. **(B)** UMAP of 16,529 cells colored by relative expression of Cd4 confirmed ILC2 populations as clusters 1 and 16. **(C)** Heatmap shows differentially expressed genes between WT and *Lyz1*$^{-/-}$ ILC2 population in cluster 16. **(D)** WT and *Lyz1*$^{-/-}$ ILC2s were partitioned and clustered. UMAP colored by relative expression of Il17rb in the 9 sub-clusters. **(E)** Bar graphs exhibited the fold enrichment and p-value for Gene ontology (GO) pathways upregulated in *Lyz1*$^{-/-}$ cluster 16 compared to WT cluster 16. **(F)** Bar graphs exhibited the fold enrichment and p-value for Gene ontology pathways upregulated in WT cluster 16 compared to *Lyz1*$^{-/-}$ cluster 16. **(G)** Representative dot blots showed the cytokine expression profile of *in vitro* cultured WT and *Lyz1*$^{-/-}$ MLN cells at steady state. Intestinal MLN cells were isolated from separately housed WT and *Lyz1*$^{-/-}$ littermates (N=2 for each genotype). **(H)** Expression pattern of cytokines secreted by WT and *Lyz1*$^{-/-}$ MLN cells cultured *in vitro* quantified and represented as bar graphs. **(I)** Quantification of pStat6 and pStat3 levels in WT and *Lyz1*$^{-/-}$ MLN cell lysates based on western blot analysis. Intestinal MLN cells were isolated from separately housed WT and KO littermates (N=2 for each genotype). All bar graphs display mean ± SEM.

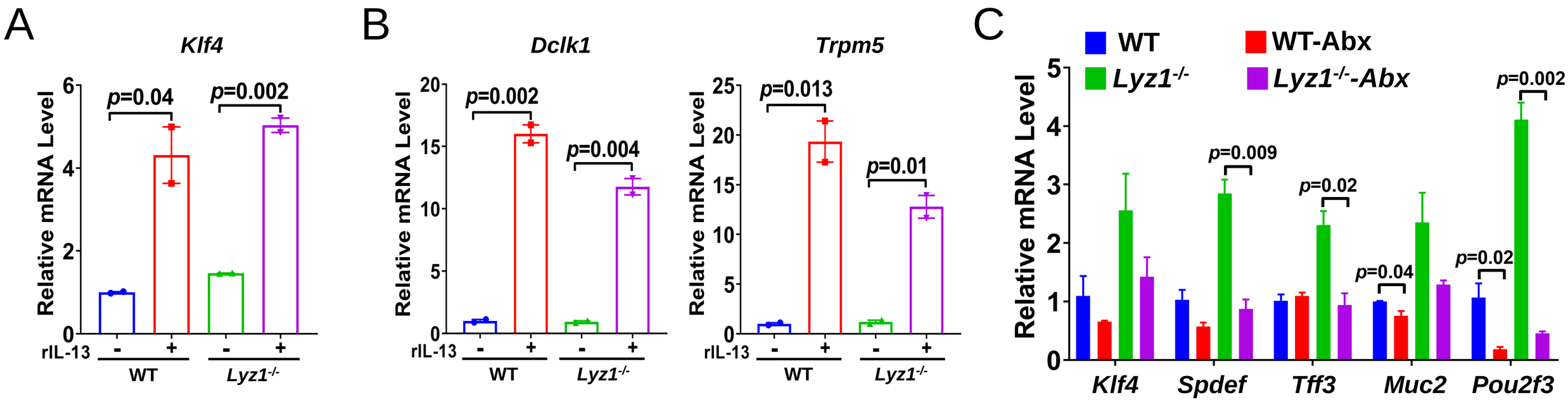
A
Klf4
Relative mRNA Level
p=0.04
p=0.002
rIL-13
WT
Lyz1-/-
B
Dclk1
p=0.002
p=0.004
Trpm5
p=0.013
p=0.01
C
WT
WT-Abx
Lyz1-/-
Lyz1-/--Abx
p=0.009
p=0.02
p=0.04
p=0.02
p=0.002
Klf4
Spdef
Tff3
Muc2
Pou2f3

Fig. S4. Type 2 immune response is non-epithelial intrinsic in *Lyz1*$^{-/-}$ mice, Related to Figure 4

(A) qPCR analysis of mRNA expression of Klf4 in ileal WT and *Lyz1*$^{-/-}$ enteroids treated with or without recombinant IL-13 (2 independent experiments). **(B)** Real-time PCR analysis of Dclk1 and Trmp5 in ileal WT and *Lyz1*$^{-/-}$ enteroids treated with or without recombinant IL-13 (2 independent experiments). **(C)** Real-time PCR analysis of goblet cell markers (Klf4, Spdef, Tff3, and Muc2) and tuft cell marker (Pou2f3) in untreated and Abs-treated WT and *Lyz1*$^{-/-}$ mice (N=4 mice for each condition). All bar graphs display mean ± SEM.

A
Alpha diversity
Ileal luminal content
Chao1 Richness
p=0.368
WT
Lyz1-/-
B
Ileal luminal content
p=0.014
Lyz1-/-
WT
CoA of alpha 0 Weighted UniFrac Distance
C
Lyz1-/-
WT
Lactobacillus_johnsonii
Eubacterium_plexicaudatum
Blautia_producta
Faecalibacterium_prausnitzii
Eubacterium_hadrum
Candidatus_Arthromitus
Ruminococcus_torques
Lactobacillus_animalis
Alistipes_putredinis
Clostridium_vincentii
Lachnoanaerobaculum_umeaense
Roseburia_faecis
Desulfovibrio_sp
Bacteroides_uniformis
Clostridium_viride
Tyzzerella_propionicum
Bifidobacterium_pseudolongum
Dorea_formicigenerans
LDA SCORE (log 10)
D
Ileal mucosal content
WT
Candidatus arthromitus
LDA SCORE (log 10)
E
441 442 443 444 445 446 447 448 449 450 451 H2O Ctrl DNA
F
Ileal Lyz1-/-
Colonic Lyz1-/-
Relative mRNA Level
p=0.052
p<0.001
p=0.002
p=0.054
WT
Lyz1-/-
TG
G
TG Line
Lysozyme
E-Cad
H
Colon
kDa
10
40
Lysozyme
β-actin
WT
TG
J
Alpha Diversity
Chao1 Richness
p=0.4
WT
TG
I
Wild type
Villin-Lyz1TG
Lysozyme
Lys E-cad DAPI
100 μm
K
Weight Change
Percentage of initial weight (%)
WT (n=5)
TG (n=10)
DSS Water
Tap water
Days of adminstration
L
Wild type
TG
3% DSS
100 μm
M
Colitis Activity
p=0.0005
Colitis score
WT
TG
N
Up in Lyz1-/-
Down in Lyz1-/-
WT vs Lyz1-/-
O
UP in TG
Down in TG
WT vs TG
P
Up in Lyz1-/-
Down in Lyz1-/-
WT vs Lyz1-/-
Q
TG
WT
Eubacterium_plexicaudatum
Parasutterella_excrementihominis
Desulfovibrio_sp
Eubacterium_ventriosum
Alistipes_putredinis
Ruminococcus_torques
Bifidobacterium_pseudolongum
Acetatifactor_muris
Clostridium_viride
Bacteroides_faecichinchillae
Lactobacillus_murinus
LDA SCORE (log 10)
R
D. formicigenerans
Abs (660nm)
Time (min)
Control
Lysozyme 20μg.mL-1
Lysozyme 200μg.mL-1
S
R. gnavus
in L-YHBHI.4
Abs (660nm)
Time (min)
T
R. gnavus
in DP2
Abs (660nm)
Time (min)
no lysozyme
lysozyme at 0h
lysozyme at 30min
lysozyme at 1h
lysozyme at 4h

Fig. S5. *Lyz1*-deficiency and –sufficiency alters composition of mucolytic composition, Related to Figure 5
(A) Chao1 index (alpha diversity) of ileal luminal microbiota in WT (N=4 mice) and *Lyz1*$^{-/-}$ (N=6 mice). **(B)** Weighted UniFrac analysis of ileal luminal microbiota from WT (in blue, N=4 mice) and *Lyz1*$^{-/-}$ mice (in green, N=6 mice). **(C)** LDA of fecal bacteria enriched in WT mice (green bars; N=14 mice) and fecal bacteria enriched in *Lyz1*$^{-/-}$ mice (red bars; N=16 mice). **(D)** LDA scores computed by LEfSe found *Candidatus Arthromitus* differentially enriched in ileal mucosal microbiota of WT mice (N=8 mice) compared to *Lyz1*$^{-/-}$ mice (N=10 mice). **(E)** Genotyping PCR confirmed TG alleles. The TG animals marked (*) were validated as founders. **(F)** qPCR analysis of lysozyme mRNA in WT, *Lyz1*$^{-/-}$, and TG ileum and colon. (N=4 for each genotype). **(G-H)** Immunostaining (N>5) **(G)** and western blot analysis (N=2 for WT and N=3 for TG) **(H)** of lysozyme in the colon of TG mice**. (I)** Immunostaining of lysozyme in WT, *Lyz1*$^{-/-}$, and TG ileum (N>5 for each genotype)**.** White arrow indicated presence of lysozyme- positive vesicles. **(J)** 16S rRNA sequencing of WT (N=6 mice) and TG (N=5 mice) analyzed for Chao1 richness showed no significant difference in alpha-diversity. **(K)** Body weight change in WT (N=5 mice) and TG (N=10 mice) littermates when treated with 3% DSS and during recovery. Dot represents mouse that died on that day. **(L-M)** Representative H. & E. images of DSS colons **(L)** and colitis activities (M) were scored from remaining 4 WT mice and 8 TG mice. **(N-P)** Phylogenetic distribution and change in relative abundance of species between WT (N=4 mice) and *Lyz1*$^{-/-}$ (N=6 mice) fecal microbiota **(N)**, WT (N=6 mice) and TG fecal microbiota (N=5 mice) **(O)**, and WT (N=4 mice) and *Lyz1*$^{-/-}$ (N=6 mice) ileal luminal microbiota **(P)**. Bar size indicates the logarithm of relative abundance fold change*. Dorea formicigenerans* and *Ruminococcus gnavus* are marked (*) in Fig S5N-P. **(Q)** LDA scores computed by LEfSe found 6 species differentially enriched in fecal microbiota of WT mice (N=6) and 5 species differentially enriched in *Lyz1*$^{-/-}$ mice (N=5). **(R)** Growth curve of *D. formicigenerans* decreased on addition of 20 µg/ml or 200 µg/ml of lysozyme during the exponential phase, when compared to the control condition. Red arrow indicated the time point of addition of lysozyme. **(S)** Growth curve of *R. gnavus* in L-YBHI.4 medium does not change on addition of lysozyme during exponential or lag phases (2-4 independent experiments). Red arrow indicated the time of addition of lysozyme.**(T)** Growth curve of *R. gnavus* in DP2 medium decreased more on addition of lysozyme 0 or 30 minutes after inoculation of culture compared to addition of lysozyme 1 or 4 hours after inoculation (2-4 independent experiments). All bar graphs display mean ± SEM.

A

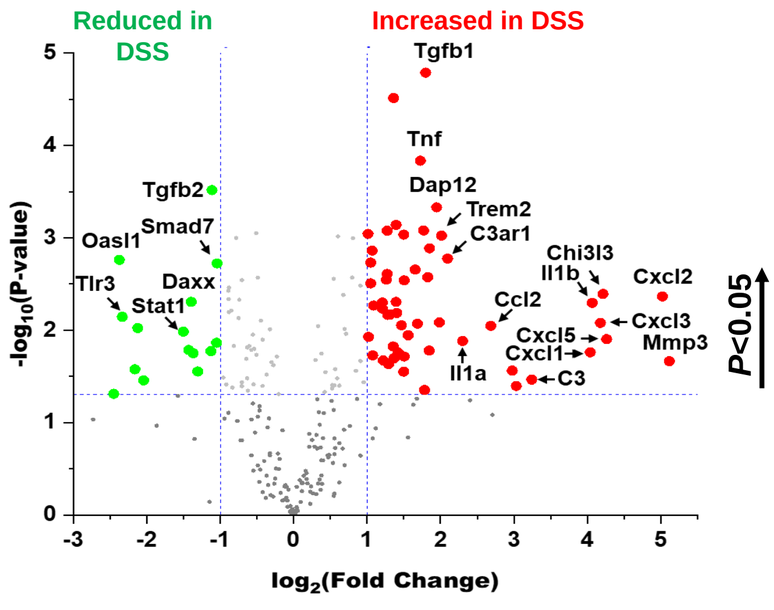
WT-FMT: DSS vs Sterile water
Reduced in DSS
Increased in DSS
-log10(P-value)
log2(Fold Change)
P<0.05
Tgfb1
Tnf
Dap12
Trem2
C3ar1
Chi3l3
Il1b
Cxcl2
Ccl2
Cxcl3
Cxcl5
Cxcl1
Mmp3
Il1a
C3
Tgfb2
Smad7
Oasl1
Tlr3
Daxx
Stat1

B

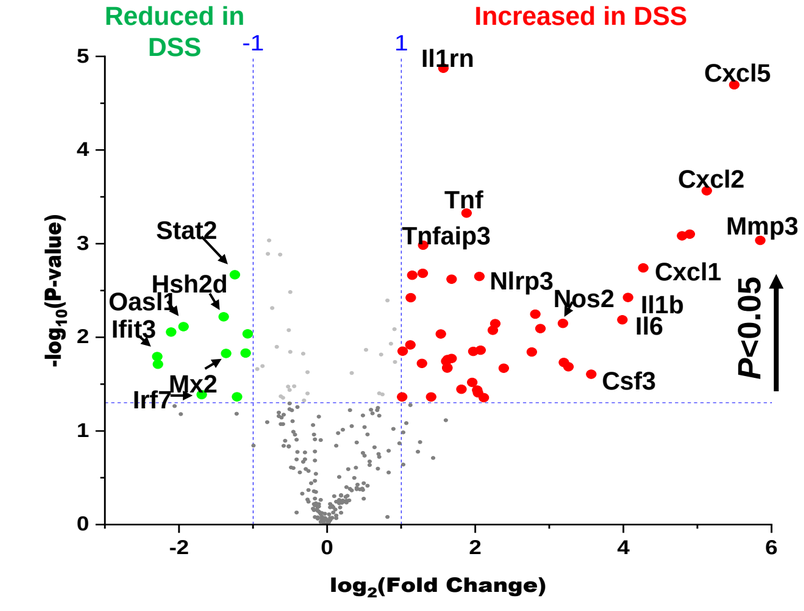
Lyz1-/--FMT: DSS vs Sterile water
Reduced in DSS
Increased in DSS
-log10(P-value)
log2(Fold Change)
P<0.05
Il1rn
Cxcl5
Cxcl2
Tnf
Tnfaip3
Mmp3
Cxcl1
Nlrp3
Nos2
Il1b
Il6
Csf3
Stat2
Hsh2d
Oasl1
Ifit3
Mx2
Irf7

C

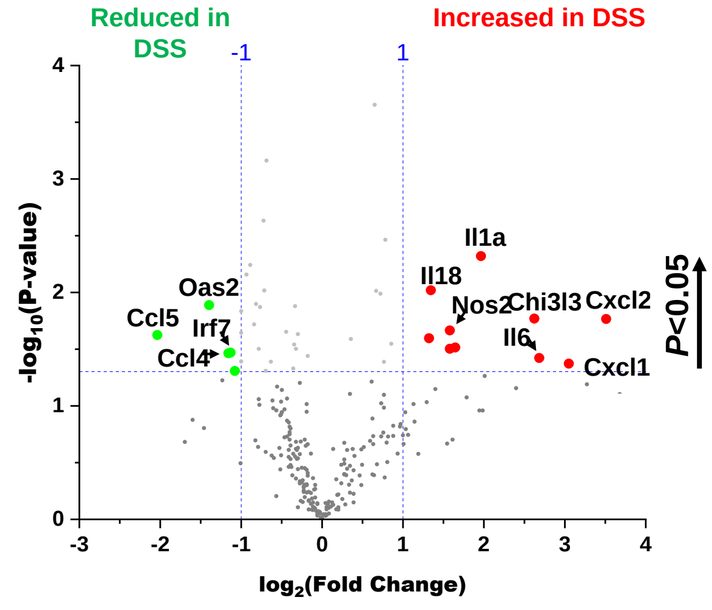
TG-FMT: DSS vs Sterile water
Reduced in DSS
Increased in DSS
-log10(P-value)
log2(Fold Change)
P<0.05
Il1a
Il18
Nos2
Chi3l3
Cxcl2
Il6
Cxcl1
Oas2
Ccl5
Irf7
Ccl4

D

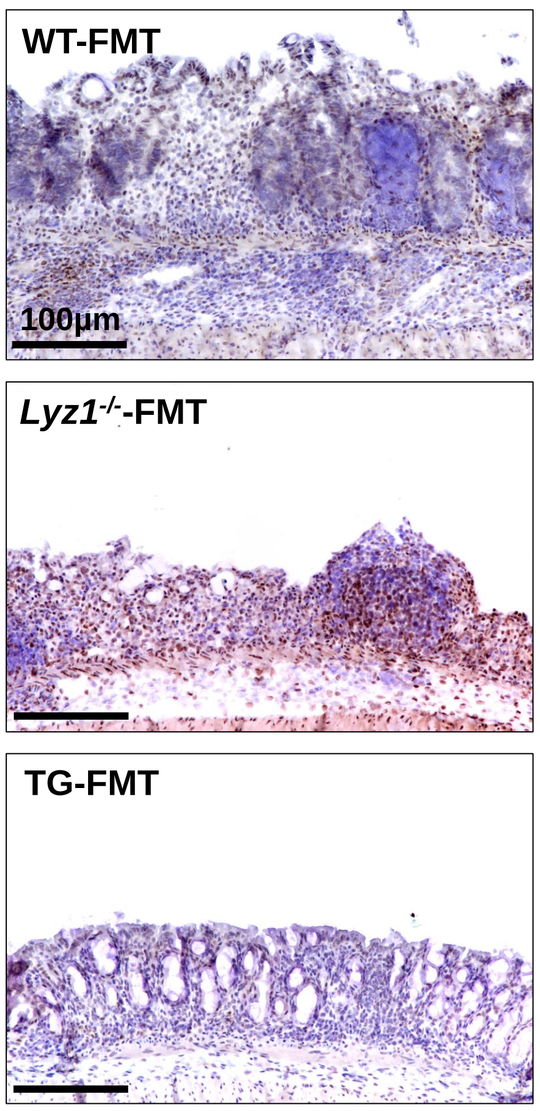
pStat3
WT-FMT
100μm
Lyz1-/--FMT
TG-FMT

E

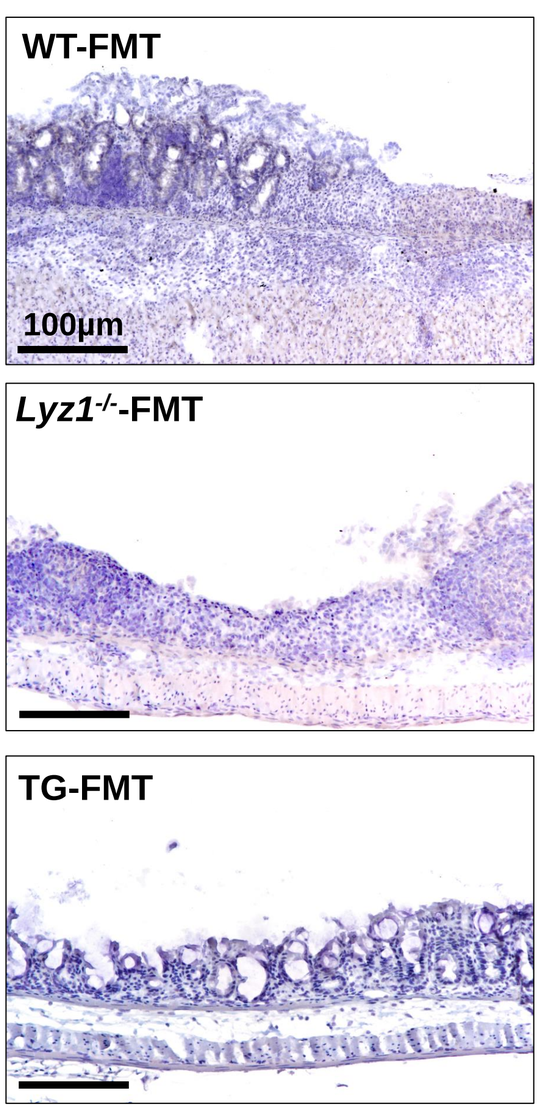
pStat6
WT-FMT
100μm
Lyz1-/--FMT
TG-FMT

F

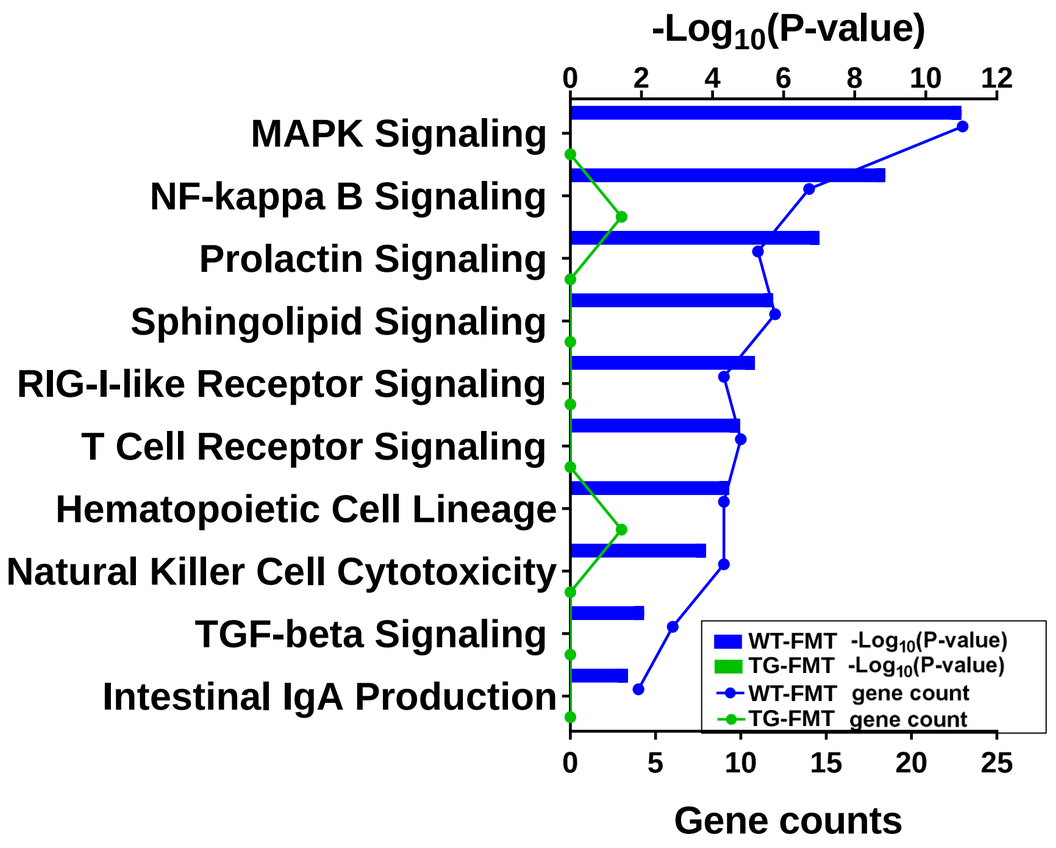
KEGG Pathway Analysis
-Log10(P-value)
MAPK Signaling
NF-kappa B Signaling
Prolactin Signaling
Sphingolipid Signaling
RIG-I-like Receptor Signaling
T Cell Receptor Signaling
Hematopoietic Cell Lineage
Natural Killer Cell Cytotoxicity
TGF-beta Signaling
Intestinal IgA Production
WT-FMT -Log10(P-value)
TG-FMT -Log10(P-value)
WT-FMT gene count
TG-FMT gene count
Gene counts

Fig. S6. Transfer of *Lyz1*$^{-/-}$ microbiota to WT GF mice does not transfer protection, Related to Figure 6
(A-C) Volcano plot of differential gene expression in DSS treatment compared to homeostasis in WT-FMT mice **(A)**, *Lyz1*$^{-/-}$ -FMT mice **(B)**, and TG-FMT mice **(C)**. Genes in red- fold change > 1; p-value < 0.05. Genes in green- fold change < -1; p-value < 0.05. N=4 mice per group at steady state and N= 5 mice per group when treated with DSS. **(D-E)** Immunostaining of phosphorylated Stat3 **(D)** and phosphorylated Stat6 **(E)** in WT-FMT, *Lyz1*$^{-/-}$ -FMT, and TG-FMT DSS-treated colon tissues (N= 5 mice per group).**(F)** KEGG Pathway analysis showed distinct differences in pathways between WT-FMT and TG-FMT, in response to DSS-induced colitis.

A

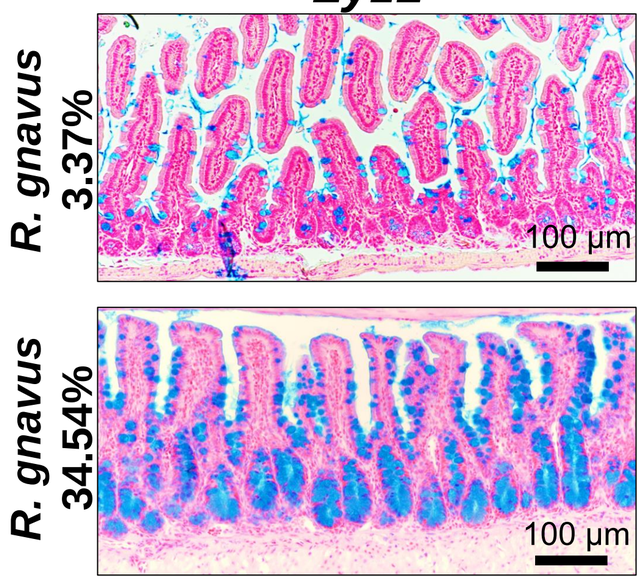

B

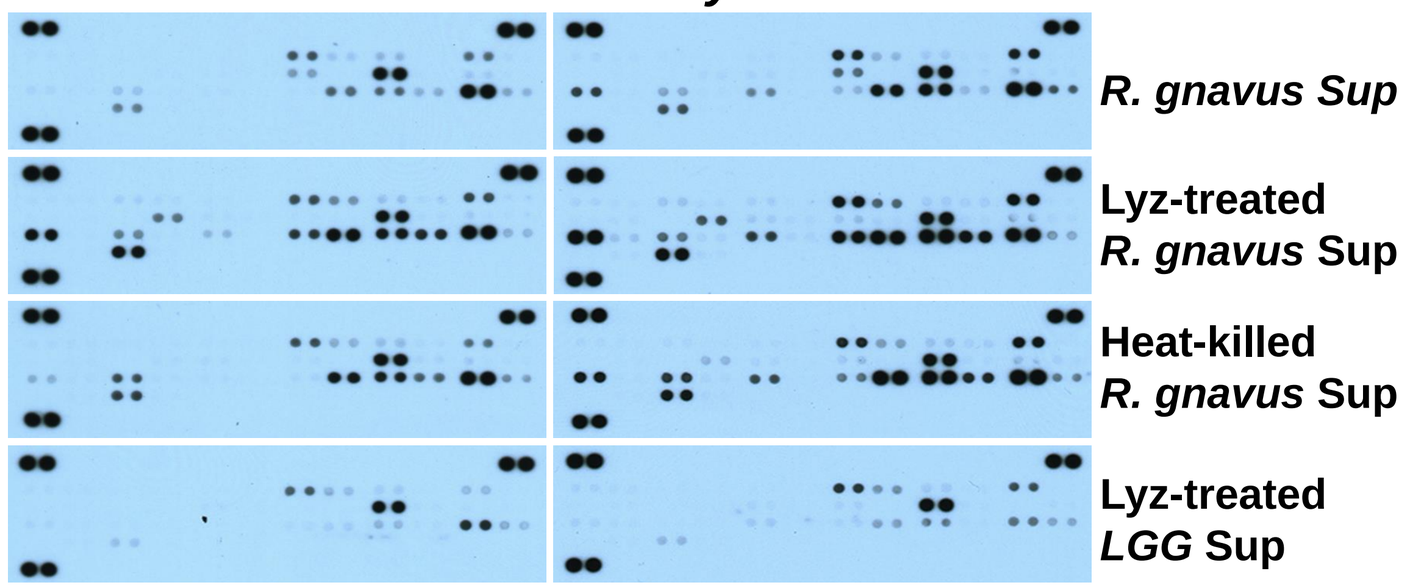

C

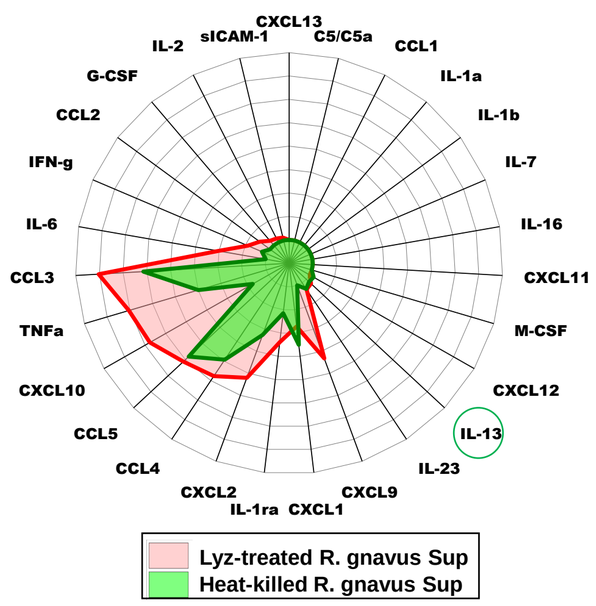

D

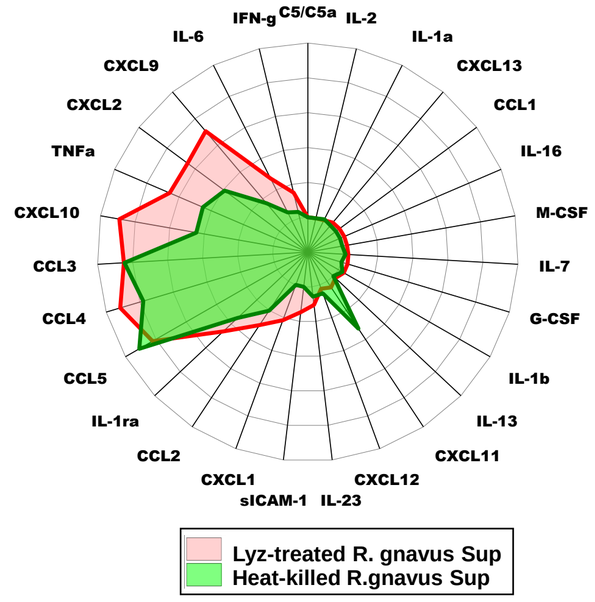

E

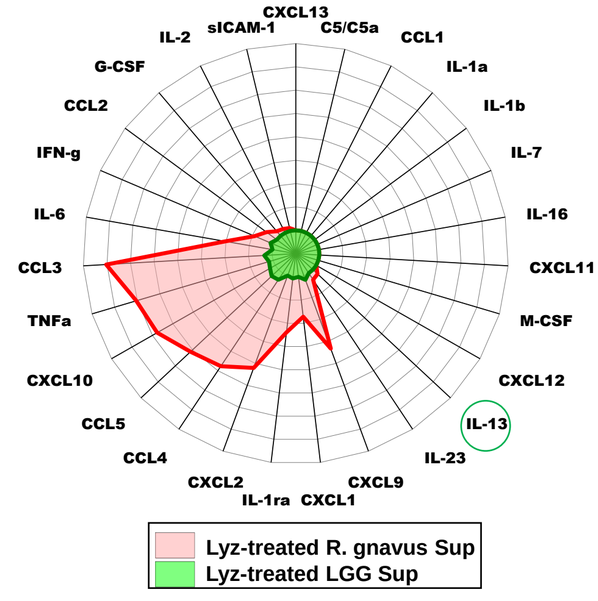

F

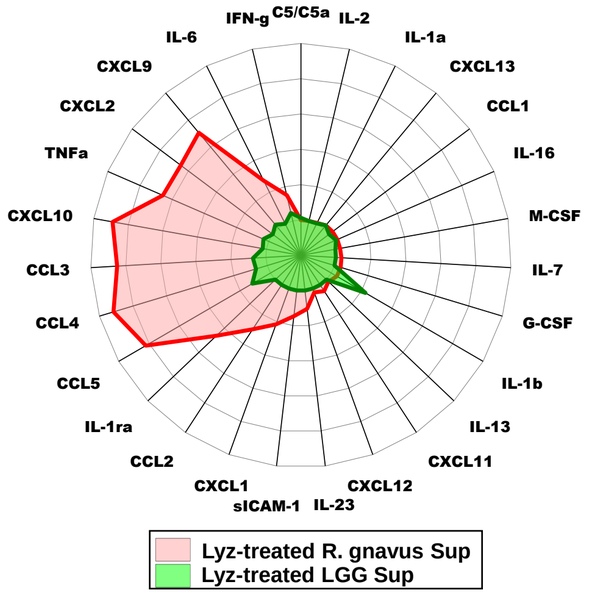

G

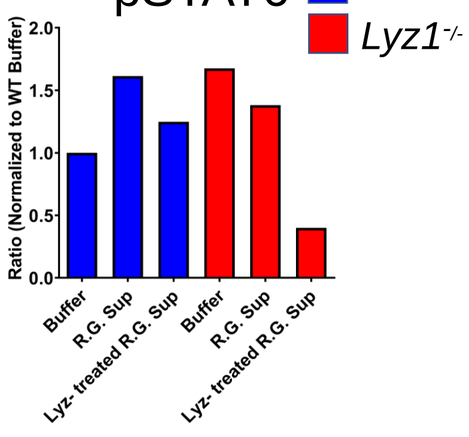

H

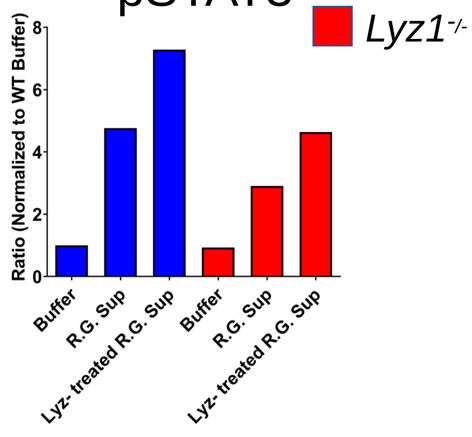

I

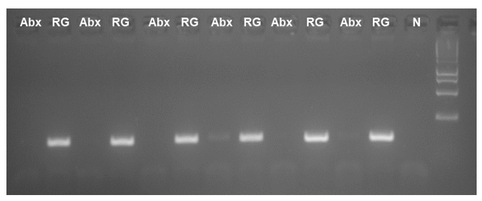

J

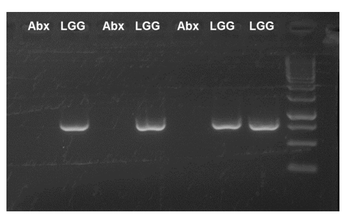

K

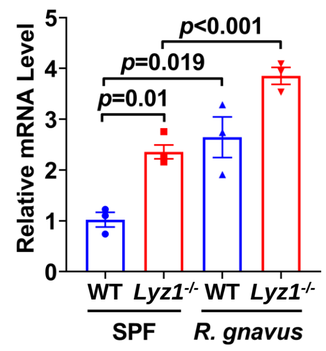

L

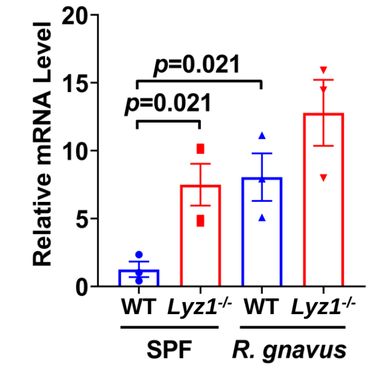

M

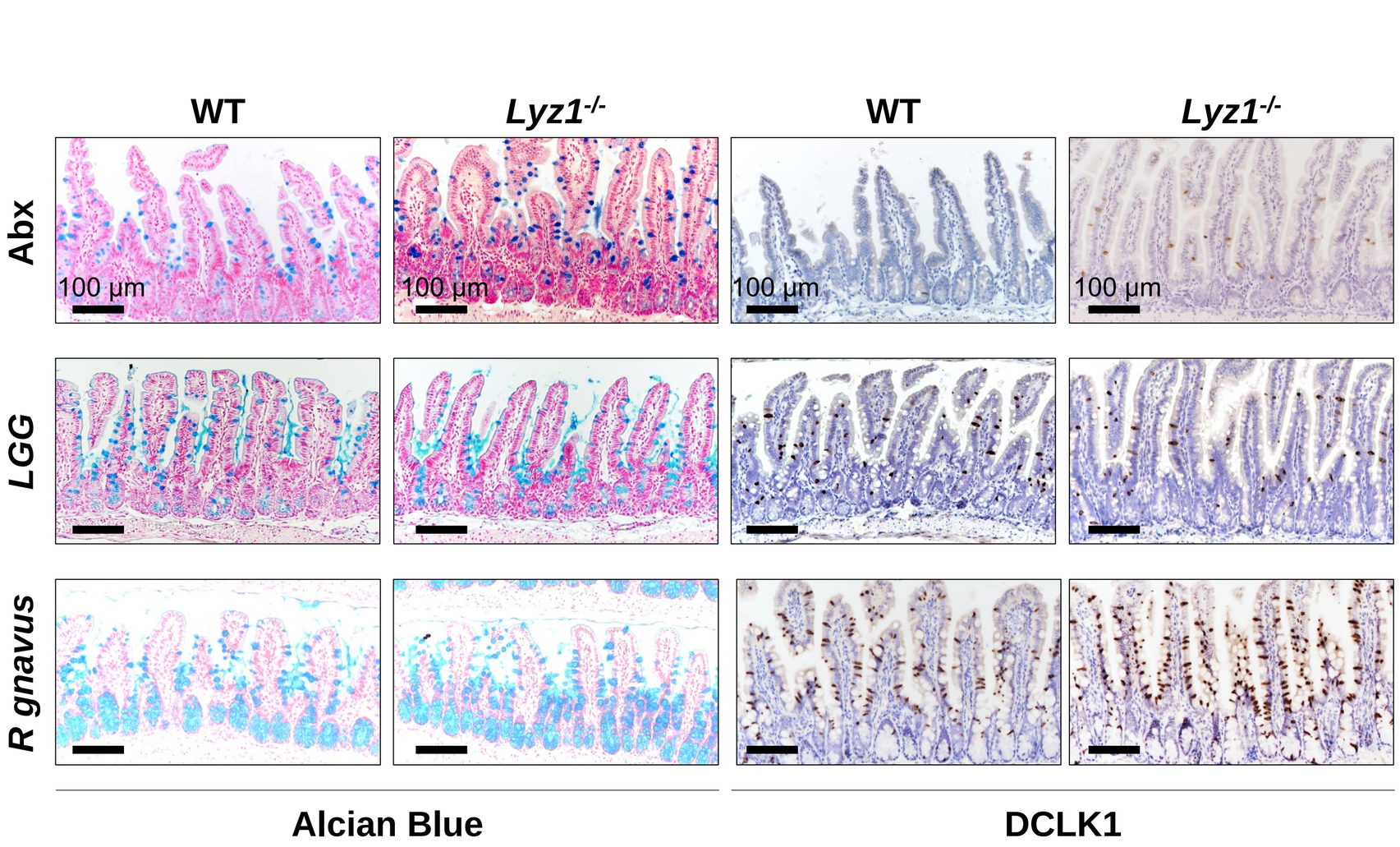

N

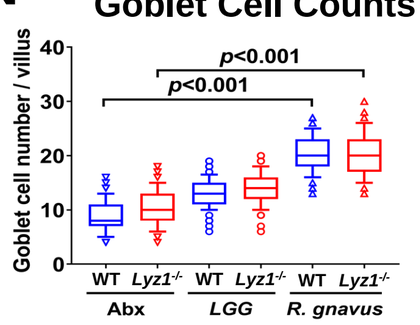

O

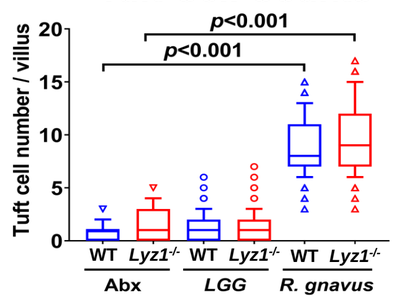

P

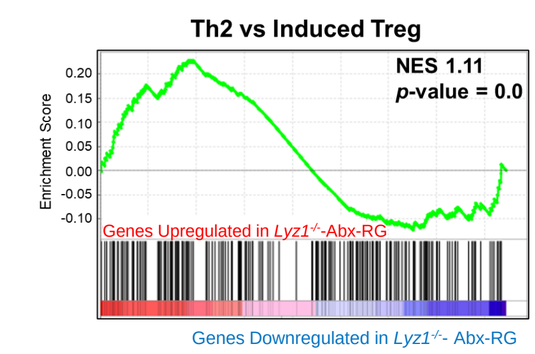

Fig. S7. Live and lysozyme-processed *R. gnavus* differentially mediates inflammatory tone, Related to Figure 7
(A) Immunostaining of Alcian blue in the small intestinal sections of *Lyz1*$^{-/-}$ mice with varying abundance of *R. gnavus*. **(B)** Representative dot blots showed the cytokine expression profile of WT and *Lyz1*$^{-/-}$ MLNs stimulated by *R. gnavus* supernatant, lysozyme-treated *R. gnavus* supernatant, heat-killed *R. gnavus* supernatant, and lysozyme- treated *LGG* supernatant. Intestinal MLN cells were isolated from separately housed WT and *Lyz1*$^{-/-}$ littermates (N=2 for each genotype) **(C-F)** Radar plots compared expression levels of cytokines in WT **(C)** and *Lyz1*$^{-/-}$ MLNs **(D)** stimulated with lysozyme-treated *R. gnavus* sup and heat-killed *R. gnavus* sup and in WT **(E)** and *Lyz1*$^{-/-}$ **(F)** MLNs treated with lysozyme-treated *R. gnavus* sup and lysozyme-treated LGG sup. Data is representative of 2 independent experiments. **(G-H)** Quantification of pSTAT6 **(G)** and pSTAT3 **(H)** levels in WT (red bars) and *Lyz1*$^{-/-}$ (blue bars) MLN cells based on western blot analysis. The values are normalized to WT buffer. **(I, J)** Semi-quantitative PCR using species-specific primer sets confirmed successful colonization of Abx-treated mice with *R. gnavus* **(I)** or *LGG* **(J)**. **(K, L)** Real-time PCR analysis of Il25 and Il13 in the ileum of SPF and *R. gnavus* colonized WT and *Lyz1*$^{-/-}$ mice. (N=3 mice per genotype per group). **(M-O)** Immunostaining of Alcian blue (goblet cells) and Dclk1 (tuft cells) **(M)** and the quantification of goblet cell **(N)** and tuft cell **(O)** numbers in antibiotics-treated, *R. gnavus* colonized, and *LGG*-colonized WT and *Lyz1*$^{-/-}$ mice (N=3 mice per genotype for Abx and *R. gnavus* group and N=2 mice per genotype for *LGG* group). Data representative of 90-100 villi per section per mouse per genotype. **(P)** GSEA of RNA-seq data comparing Th2 signature in *R. gnavus* colonized *Lyz1*$^{-/-}$ mice and *R. gnavus* colonized WT mice (N=3 mice per genotype). All bar graphs display mean ± SEM.

Name	WT=4 vs. *Lyz1*$^{-/-}$=8	WT=6 vs. TG=5
Akkermansia muciniphila	UP in *Lyz1*$^{-/-}$	Down in TG
Anaerotruncus colihominis	UP in *Lyz1*$^{-/-}$	Down in TG
Clostridium sp	UP in *Lyz1*$^{-/-}$	Down in TG
Dorea formicigenerans	UP in *Lyz1*$^{-/-}$	Down in TG
Eubacterium plexicaudatum	UP in *Lyz1*$^{-/-}$	Down in TG
Lactobacillus reuteri	UP in *Lyz1*$^{-/-}$	Down in TG
Lactobacillus vaginalis	UP in *Lyz1*$^{-/-}$	Down in TG
Marvinbryantia formatexigens	UP in *Lyz1*$^{-/-}$	Down in TG
Moryella indoligenes	UP in *Lyz1*$^{-/-}$	Down in TG
Mucispirillum schaedleri	UP in *Lyz1*$^{-/-}$	Down in TG
Oscillibacter sp.	UP in *Lyz1*$^{-/-}$	Down in TG
Oscillibacter valericigenes	UP in *Lyz1*$^{-/-}$	Down in TG
Ruminococcus gnavus	UP in *Lyz1*$^{-/-}$	Down in TG
Acetatifactor muris	UP in *Lyz1*$^{-/-}$	UP in TG
Bifidobacterium pseudolongum	UP in *Lyz1*$^{-/-}$	UP in TG
Parvibacter caecicola	UP in *Lyz1*$^{-/-}$	UP in TG
Tyzzerella propionicum	UP in *Lyz1*$^{-/-}$	UP in TG
Clostridium viride	UP in *Lyz1*$^{-/-}$	UP in TG
Alistipes finegoldii	UP in *Lyz1*$^{-/-}$	UNCHANGED in TG
Anaerostipes butyraticus	UP in *Lyz1*$^{-/-}$	UNCHANGED in TG
Anaerostipes sp	UP in *Lyz1*$^{-/-}$	UNCHANGED in TG
Bacteroides sp	UP in *Lyz1*$^{-/-}$	UNCHANGED in TG
Bacteroides uniformis	UP in *Lyz1*$^{-/-}$	UNCHANGED in TG
Coprococcus eutactus	UP in *Lyz1*$^{-/-}$	UNCHANGED in TG
Eubacterium hadrum	UP in *Lyz1*$^{-/-}$	UNCHANGED in TG
Eubacterium ramulus	UP in *Lyz1*$^{-/-}$	UNCHANGED in TG
Faecalibacterium prausnitzii	UP in *Lyz1*$^{-/-}$	UNCHANGED in TG
Helicobacter cf	UP in *Lyz1*$^{-/-}$	UNCHANGED in TG
Helicobacter equorum	UP in *Lyz1*$^{-/-}$	UNCHANGED in TG
Helicobacter ganmani	UP in *Lyz1*$^{-/-}$	UNCHANGED in TG
Helicobacter sp	UP in *Lyz1*$^{-/-}$	UNCHANGED in TG
Lachnoanaerobaculum umeasense	UP in *Lyz1*$^{-/-}$	UNCHANGED in TG
Oscillospira guilliermondii	UP in *Lyz1*$^{-/-}$	UNCHANGED in TG
Ruminococccus gauvreauii	UP in *Lyz1*$^{-/-}$	UNCHANGED in TG
Ruminococcus faecis	UP in *Lyz1*$^{-/-}$	UNCHANGED in TG
Stomatobaculum longum	UP in *Lyz1*$^{-/-}$	UNCHANGED in TG

Table. S1. Thirty-six species increased in *Lyz1*$^{-/-}$ mouse fecal microbiota. WT (N=4) vs. *Lyz1*$^{-/-}$ (N=8); WT (N=6) vs.TG (N=5), Related to Figure 5.

Ranked by *Lyz1*$^{-/-}$ %	Name	WT (%)	*Lyz1*$^{-/-}$ (%)	FC (by %)	WT (Counts)	*Lyz1*$^{-/-}$ (Counts)	FC (by Counts)
1	Ruminococcus gnavus	3.66	6.01	1.64	81498	284916	3.50
2	Clostridium sp.	1.00	1.43	1.43	22233	67840	3.05
3	Lactobacillus vaginalis	0.11	0.18	1.67	2400	8539	3.56
4	Dorea formicigenerans	0.02	0.14	8.94	351	6680	19.03
5	Mucispirillum schaedleri	0.03	0.12	4.14	644	5674	8.81
6	Akkermansia muciniphila	0.05	0.06	1.12	1206	2864	2.37
7	Lactobacillus reuteri	0.03	0.06	1.72	736	2689	3.65
8	Moryella indoligenes	0.02	0.02	1.16	459	1129	2.46
9	Oscillibacter sp.	0.00	0.02	4.73	104	1047	10.07
10	Eubacterium plexicaudatum	0.00	0.02	45.00	10	958	95.80
11	Oscillibacter valericigenes	0.00	0.01	3.62	71	547	7.70
12	Anaerotruncus colihominis	0.00	0.00	4.70	22	220	10.00
13	Marvinbryantia formatexigens	0.00	0.00	NA	0	62	NA

Ranked by WT %	Name	WT (%)	TG (%)	FC (by %)	WT (Counts)	TG (Counts)	FC (by Counts)
1	Ruminococcus gnavus	1.72	1.19	0.69	81278	38622	0.48
2	Clostridium sp.	0.83	0.53	0.64	39367	17278	0.44
3	Mucispirillum schaedleri	0.18	0.02	0.12	8743	733	0.08
4	Dorea formicigenerans	0.04	0.01	0.25	1898	321	0.17
5	Lactobacillus vaginalis	0.03	0.03	0.81	1500	833	0.56
6	Oscillibacter valericigenes	0.03	0.01	0.24	1346	219	0.16
7	Akkermansia muciniphila	0.02	0.01	0.22	1128	172	0.15
8	Oscillibacter sp.	0.01	0.01	0.57	496	193	0.39
9	Moryella indoligenes	0.01	0.01	0.74	340	174	0.51
10	Lactobacillus reuteri	0.01	0.00	0.48	326	107	0.33
11	Anaerotruncus colihominis	0.01	0.00	0.46	281	88	0.31
12	Eubacterium plexicaudatum	0.00	0.00	0.00	140	0	0.00
13	Marvinbryantia formatexigens	0.00	0.00	NA	13	0	NA

Table. S2. Thirteen species that increased in *Lyz1*$^{-/-}$ and decreased in TG mice were ranked by their abundance (%) in *Lyz1*$^{-/-}$ fecal microbiota. WT (N=4) vs. *Lyz1*$^{-/-}$ (N=8); WT (N=6) vs. TG (N=5), Related to Figure 5.

.

		Fecal microbiota						Ileum luminal microbiota		
Ranked by Fecal KO %	Species	WT (%)	*Lyz1*$^{-/-}$ (%)	FC	WT (%)	TG (%)	FC	WT (%)	*Lyz1*$^{-/-}$ (%)	FC
1	*R. gnavus*	3.66	6.01	1.64	1.72	1.19	0.69	0.00	0.39	>39
2	*Clostridium sp.*	1.00	1.43	1.43	0.83	0.53	0.64	0.031	0.296	9.68
3	*L. vaginalis*	0.11	0.18	1.67	0.032	0.026	0.81	1.63	0.61	0.38
4	*D. formicigenerans*	0.02	0.14	8.94	0.04	0.01	0.25	0.004	0.05	14.34
5	*M. schaedleri*	0.03	0.12	4.14	0.18	0.02	0.12	0.00	1.14	>114
6	*A. muciniphila*	0.05	0.06	1.12	0.02	0.01	0.22	0.0003	0.0008	2.71
7	*L. reuteri*	0.03	0.06	1.72	0.01	0.003	0.48	0.40	0.23	0.57
8	*M. indoligenes*	0.02	0.02	1.16	0.007	0.005	0.74	0.0012	0.0010	0.86
9	*Oscillibacter sp.*	0.005	0.02	4.73	0.010	0.006	0.57	0.00	0.00	N/D

Table. S3. Bacteria increased in *Lyz1*$^{-/-}$ and decreased in TG mice, Related to Figure 5.

Name	Fecal	Ileal luminal
Acetatifactor muris	Up in *Lyz1*$^{-/-}$	Up in *Lyz1*$^{-/-}$
Bifidobacterium pseudolongum	Up in *Lyz1*$^{-/-}$	Up in *Lyz1*$^{-/-}$
Clostridium viride	Up in *Lyz1*$^{-/-}$	Up in *Lyz1*$^{-/-}$
Coprococcus eutactus	Up in *Lyz1*$^{-/-}$	Up in *Lyz1*$^{-/-}$
Dorea formicigenerans	Up in *Lyz1*$^{-/-}$	Up in *Lyz1*$^{-/-}$
Eubacterium hadrum	Up in *Lyz1*$^{-/-}$	Up in *Lyz1*$^{-/-}$
Faecalibacterium prausnitzii	Up in *Lyz1*$^{-/-}$	Up in *Lyz1*$^{-/-}$
Helicobacter cf	Up in *Lyz1*$^{-/-}$	Up in *Lyz1*$^{-/-}$
Helicobacter ganmani	Up in *Lyz1*$^{-/-}$	Up in *Lyz1*$^{-/-}$
Mucispirillum schaedleri	Up in *Lyz1*$^{-/-}$	Up in *Lyz1*$^{-/-}$
Oscillibacter valericigenes	Up in *Lyz1*$^{-/-}$	Up in *Lyz1*$^{-/-}$
Ruminococcus gnavus	Up in *Lyz1*$^{-/-}$	Up in *Lyz1*$^{-/-}$
Tyzzerella propionicum	Up in *Lyz1*$^{-/-}$	Up in *Lyz1*$^{-/-}$
Clostridium sp	Up in *Lyz1*$^{-/-}$	Up in *Lyz1*$^{-/-}$
Akkermansia muciniphila	Up in *Lyz1*$^{-/-}$	Unchanged
Eubacterium ramulus	Up in *Lyz1*$^{-/-}$	Unchanged
Helicobacter equorum	Up in *Lyz1*$^{-/-}$	Unchanged
Helicobacter sp	Up in *Lyz1*$^{-/-}$	Unchanged
Marvinbryantia formatexigens	Up in *Lyz1*$^{-/-}$	Unchanged
Oscillibacter sp.	Up in *Lyz1*$^{-/-}$	Unchanged
Ruminococccus gauvreauii	Up in *Lyz1*$^{-/-}$	Unchanged
Bacteroides uniformis	Up in *Lyz1*$^{-/-}$	Unchanged
Lactobacillus reuteri	Up in *Lyz1*$^{-/-}$	Unchanged
Lactobacillus vaginalis	Up in *Lyz1*$^{-/-}$	Unchanged
Moryella indoligenes	Up in *Lyz1*$^{-/-}$	Unchanged
Parvibacter caecicola	Up in *Lyz1*$^{-/-}$	Unchanged
Alistipes finegoldii	Up in *Lyz1*$^{-/-}$	N/D
Anaerostipes butyraticus	Up in *Lyz1*$^{-/-}$	N/D
Anaerostipes sp	Up in *Lyz1*$^{-/-}$	N/D
Anaerotruncus colihominis	Up in *Lyz1*$^{-/-}$	N/D
Bacteroides sp	Up in *Lyz1*$^{-/-}$	N/D
Eubacterium plexicaudatum	Up in *Lyz1*$^{-/-}$	N/D
Lachnoanaerobaculum umeasense	Up in *Lyz1*$^{-/-}$	N/D
Oscillospira guilliermondii	Up in *Lyz1*$^{-/-}$	N/D
Ruminococcus faecis	Up in *Lyz1*$^{-/-}$	N/D
Stomatobaculum longum	Up in *Lyz1*$^{-/-}$	N/D

Table. S4. Thirty-six species increased in *Lyz1*$^{-/-}$ mouse fecal microbiota. WT (N=4) vs. *Lyz1*$^{-/-}$ (N=8) Fecal microbiota; WT (N=4) vs. *Lyz1*$^{-/-}$ (N=6) ileal luminal content, Related to Figure 5.

Ranked by WT %	Species	WT (%)	TG (%)	FC (by %)	WT (Counts)	TG (Counts)	FC (by Counts)
1	Lactobacillus murinus	0.09	0.43	5.05	4079	14144	3.47
2	Candidatus Arthromitus	0.02	0.02	1.19	873	716	0.82
3	Lactobacillus animalis	0.01	0.02	1.64	587	663	1.13
4	Clostridium perfringens	0.00	0.01	8.16	61	342	5.61
5	Enterorhabdus caecimuris	0.00	0.01	4.72	53	172	3.25
6	Roseburia faecis	0.00	0.00	7.22	24	119	4.96
7	Enterorhabdus mucosicola	0.00	0.00	1.19	65	53	0.82

Ranked by TG %	Species	WT (%)	*Lyz1*$^{-/-}$ (%)	FC (by %)	WT (Counts)	*Lyz1*$^{-/-}$ (Counts)	FC (by Counts)
1	Roseburia faecis	0.17	0.07	0.41	3747	3253	0.87
2	Lactobacillus murinus	0.13	0.05	0.37	3004	2361	0.79
3	Clostridium perfringens	0.10	0.02	0.17	2158	777	0.36
4	Enterorhabdus caecimuris	0.04	0.02	0.60	881	1126	1.28
5	Candidatus Arthromitus*	0.04	0.00	NA	3646	63	0.02
6	Lactobacillus animalis	0.03	0.00	0.15	649	208	0.32
7	Enterorhabdus mucosicola	0.00	0.00	0.00	13	0	0.00

Table. S5. Seven species increased in TG and decreased in *Lyz1*$^{-/-}$ mice. WT (N=6) vs. TG (N=5); WT (N=4) vs. *Lyz1*$^{-/-}$ (N=8), Related to Figure 5.

	L-YHBHI.4 Concentration (g/L)	L-YHBHI.4 + mucin Concentration (g/L)	DP2 Concentration (g/L)
Brain Heart Infusion	37	37	-
Yeast Extract	5	5	-
Maltose	0,50	0,50	-
Cellobiose	0,50	0,50	-
Starch	0,50	0,50	-
Mucin type II	-	1	-
L-Cystéine-HCl	0,5	0,5	0.5
Hemin 0.5%	0.005	0.005	0.005
Resazurin solution 0.1%	0.004	0.004	0.004
Meat extract			5
Sodium Pyruvate			1
Sodium Succinate			5
Bactopeptone			5
$CaCl_2$, $2H_2O$			0.01
KH_2PO_4			0.04
K_2HPO_4			0.04
NaCl			0.08
$ZnSO_4$, $7H_20$			0.02
$NaHCO_3$			0.4
Vitamins			
-K1			1.10^{-6}
-B1			5.10^{-5}
-B2			5.10^{-5}
-B8			2.10^{-5}

Table. S6. Detailed composition of the bacteria culture media used *Ruminococcus gnavus*, Related to STAR Methods.

Gene name	Forward primer	Reverse primer
Dorea formicigenerans	GCAGCTAACGCAATAAGCAG	CTTCCATTACGAAGCGGTC
Ruminococcus gnavus	GGACTGCATTTGGAACTGTCAG	AACGTCAGTCATCGTCCAGAAAG
Bacterial 16s rRNA	ACTACGTGCCAGCAGCC	GGACTACCAGGGTATCTAATCC
Tritrichomonas muris	GCTTTTGCAAGCTAGGTCCC	TTTCTGATGGGGCGTACCAC
Mouse Lyz1	ATGGCTACCGTGGTGTCAAG	CGGTCTCCACGGTTGTAGTT
Mouse Mucin 2 (Muc2)	TGTGTGGGACCTGACAATGT	CACACAATGCCACTTCCACC
Mouse Klf4	CACACCTGCGAACTCACAC	GGTAGTGCCTGGTCAGTTCA
Mouse Spdef	CTATGGCCGCTTCATCCGCT	GTTCTTGCGCACACCCCAC
Mouse Il4	AGTGTTCTCATGGAGCTGCA	CAGTGATGTGGACTTGGACTCA
Mouse Il13	CGGTGCCAAGATCTGTGTCT	ACACTCCATACCATGCTGCC
Mouse Il17a	GTTCCACGTCACCCTGGACT	CTTTCCCTCCGCATTGACAC
Mouse Il17f	ACGTGAATTCCAGAACCGCT	TGATGCAGCCTGAGTGTCTG
Mouse Il25	ACACCCACCACGCAGAAT	ACCCGATTCAAGTCCCTGTC
Mouse Il33	TGGGAAGAAGCTGATGGTGA	CGAGACGTCACCCCTTTGAA
Mouse Tslp	CCTTCACTCCCCGACAAAAC	TGCCATTTCCTGAGTACCGT
Mouse Tnfa	ACAAGCCTGTAGCCCACGTC	CTTTGAGATCCATGCCGTTG
Mouse Pou2f3	ACCCATCTACAACTCCCGGC	CCAGGGGAACAGGATGACGT
Mouse Gata3	GAGGAGGAACGCTAATGGGG	CGGGTCTGGATGCCTTCTTT
Mouse Tbx21 (Tbx)	GGCTTCCAACAATGTGACCC	TGTTAGAAGCACTGCAGGCA
Mouse Rorc (Rorγt)	GTGTGCTGTCCTGGGCTAC	CCCAGATGACTTGTCCCCAC
Mouse Foxp3	TGGAAAAGGAGAAGCTGGGAG	AGTACTGGTGGCTACGATGC
Mouse Tgfb1	CGGAGAGCCCTGGATACCA	CTTCCAACCCAGGTCCTTCC
Mouse Amphiregulin (Areg)	CGGCATCGTTATCACAGTGC	TGCACAGTCCCGTTTTCTTG
Mouse Hprt	TCCCTGGTTAAGCAGTACAGC	TCCAACAAAGTCTGGCCTGT

Table. S7. Primer list for quantitative RT-PCR, Related to STAR Methods.